Progress of Theoretical Physics, Vol. 116, No. 4, October 2006

Correlated EoM and Distributions for $A = 6$ Nuclei

M. Tomaselli,[1,2] T. Kühl,[2] D. Ursescu[2] and S. Fritzsche[3]

[1]*Institute of Physics, Darmstadt University, D-64289 Darmstadt, Germany*
[2]*GSI Gesellschaft für Schwerionenforschung, D-64291 Darmstadt, Germany*
[3]*Institute of Physics, Kassel University, D-34132 Kassel, Germany*

(Received March 27, 2006)

Energy spectra and electromagnetic transitions of nuclei are strongly depending from the correlations of the bound nucleons. Two particle correlations are responsible for the scattering of model particles either to low momentum- or to high momentum-states. The low momentum states form the model space while the high momentum states are used to calculate the G-matrix. The three and higher order particle correlations do not play a role in the latter calculation especially if the correlations induced by the scattering operator are of sufficient short range. They modify, however, via the long tail of the nuclear potential, the Slater determinant of the A particles by generating excited Slater's determinants. In this work the influence of the correlations on the level structure and ground state distributions of even open shell nuclei is analyzed via the boson dynamic correlation model BDCM. The model is based on the unitary operator e^S (S is the correlation operator) formalism which in this paper is presented within a non-perturbative approximation. The low lying spectrum calculated for ^{6}Li reproduces very well the experimental spectrum while for ^{6}He a charge radius slightly larger than that obtained within the isotopic-shift (IS) theory has been calculated. Good agreement between theoretical and experimental results has been obtained without the introduction of a genuine three body force.

§1. Introduction

Correlation effects in nuclei have been first introduced in nuclei by Villars,[1)] who proposed the unitary-model operator (UMO) to construct effective operators. The method was implemented by Shakin[2)] for the calculation of the G-matrix from hard-core interactions. Non-perturbative approximations of the UMO have been recently applied to even nuclei in Ref. 3) which here is treated in more detail. The basic formulas of the Boson Dynamic Correlation Model (BDCM) presented in the above quoted paper have been obtained by solving the n-body problem in the following approximations:

a) The n-body correlation operator is separated in short- and long-range components. The short-range component is considered up to the two body correlation while for the long-range component the three and four body correlation operators have been studied. The extension of the correlation operator to high order diagrams is especially important in the description of exotic nuclei (open shell). In the short range approximation the model space of two interacting particles is separated in two subspaces: one which includes the shell model states and the other (high momentum) which is used to compute the G-matrix of the model. The long-range component of the correlation operator has the effect of generating a new correlated model space (effective space) which departs from the originally adopted one (shell model). The

amplitudes of the model wave functions are calculated in terms of nonlinear equation of motions (EoM),
b) the n-body matrix elements are calculated exactly via the Cluster Factorization Theory (CFT),
c) by linearizing the systems of commutator equations, which characterize the EoM. The generalized linearization approximations (GLA) includes in the calculation presented in the paper up to the (3p1h) effective diagrams. The linearized terms are not discarded but provide, as explained later in the text, the additional matrix elements that convert the perturbative UMO expansion in an eigenvalue equation.

Within the present treatment of the correlation operator one generates in the n-body theory not only the ladder diagrams of Ref. 4) but also the folded diagrams of Kuo.[5)]

In this paper the BDCM model is applied to calculate the influence of the correlations on the energy spectrum of ^{6}Li and on the charge distributions of ^{6}He and ^{6}Li. The motivation of these calculations relies from one side in the study the effect of the correlation operator on the theoretical charge radius of ^{6}He and from the other side in investigating the variation of the charge distribution and magnetic moment of the ground state of ^{6}Li under the variation of the adopted model space.

The value obtained for the charge radius of the correlated ^{6}He is slightly bigger than the radius calculated in other theories[6),9)] and that derived within the isotopic-shift IS theory.[10)] A charge radius which agrees with the radii calculated in Refs. 6) and 9), and those calculated in the cluster models of Refs. 11)–13) is on the other hand obtained by considering only two protons in the $1s_{\frac{1}{2}}$. This non-correlated radius agrees also with the radius derived at Argonne within the IS theory.[10)] Correlations have therefore the property to increase the charge radius of ^{6}He as observed for the isotopes of Lithium.

The calculations performed in Ref. 14) for the charge radii of the lithium isotopes, although in good agreement with those measured at GSI-TRIUMF[15)] and analyzed with the help of Ref. 16), are always slightly larger than those measured. For the stable isotope ^{6}Li the calculated radius agrees with the value obtained with the electron scattering experiments of Ref. 17). However, the charge radii calculated in the IS theory could also depend on the nuclear correlations. The consideration of the microscopic correlations as presented in this paper will generate a new evaluation procedure for the Mass Shift (MS) and the Field Shift (FS). As a result, both quantities could be evaluated within non-perturbative methods which include the nuclear effects.

The importance of the correlations in the evaluation of the FS has already been pointed out in Ref. 19) where we calculate the FS of ^{7}Li and show that the departure from a point nuclear approximation is rather a big effect. Additionally the higher order cross term contributions of Ref. 18) need to be considered. A direct comparison between the calculated and the measured charge radii should be therefore performed after an accurate analysis of these two correcting factors.

Theoretically the effect of the correlation on the distributions of medium-heavy nuclei has already been performed in Refs. 20)–22) within a phenomenological corre-

lation model. In light nuclei, however, the calculation of distributions performed by the theoretical models of Refs. 6)–9) has been done in terms of non-correlated particles. In Refs. 6) and 7), and references therein, a large-basis no-core shell model has been used. In this model the e^S method is considered up to the "two body cluster approximation". Within this approximation the effective interaction obtained contains no hole state. This will be, however, not the case by expanding the e^S method to higher cluster approximations as done in the present paper. Unstable nuclei have been described by the antisymmetrized molecular dynamics (AMD) of Ref. 8) neglecting correlations. Quantum Monte Carlo calculations have been performed by using realistic nuclear Hamiltonians that fit nucleon-nucleon scattering data in light nuclei.[9] Good results have been obtained for structure calculations, but the model cannot introduce correlated wave functions in the calculation of the distributions.

Another important argument for the consideration of correlation effects comes from the analysis of the magnetic moments. The magnetic moment of the ground state of ^{6}Li calculated in a model base in which the hole is confined to the $1s_{\frac{1}{2}}$ is smaller than the experimental value. Only with the use of a large configuration base, which includes the spin-flip component $1p_{\frac{3}{2}}^{-1}1p_{\frac{1}{2}}$ proposed by Arima[23] we obtain a very good value for the magnetic moment. The large configuration base has also the effect of decreasing the energy of the second 1^- level.

§2. Theory of correlated two particle systems

The effect of the correlations between nucleons in open shell nuclei is investigated within a system of coupled commutator equations, which via the GLA Ansatz, is converted in an eigenvalue equation. These describe a situation in which valence particles and core-excited states are coexisting. The advantage of this model is to provide larger effective configuration spaces (see Appendix A) than that used in the shell model calculation, to include exactly the Pauli principle in the coupled spaces, and to generate correlated solutions for the $n \equiv$ paired systems.

We start by computing the commutator of the valence particles with the nuclear Hamilton operator. In this calculation we retain the linear (shell model) terms with dimension n and nonlinear (valence pairs coupled to one particle-hole pair) excitations with dimension $n + 1'$. The $1'$ denotes one particle-hole pair. In the next equation we have then to take care of the nonlinear terms derived in the first step. The commutator of the Hamilton operator with the $n + 1'$ excited states generates the coupling of the n-valence pairs to two particles-holes (2p-2h) excitations with dimension $n + 2'$. The successive equations are then characterizing the commutators which involve valence particles coupled to an increasing number of particle-hole pairs $n + n'$. It is worthwhile to remark that the obtained system of commutator equations is similar to the chain of equations one derives within the Green function dynamics of Ref. 9). The introduced computational steps describe the mixing of the shell model states to core excitations with an increasing degree of complexity which will find applications in the calculation of the structures of exotic nuclei. This commutator chain is suitable to be solved perturbatively by inserting the n-th commutator in

the $(n-1)$-th commutator, $(n-1)$-th commutator in the $(n-2)$-th commutator, ... the second commutator in the first. Within this perturbative approach one defines effective Hamiltonians of the model which, due to the increasing degree of complexity, are not easily solvable. Much simpler solutions to the commutator equations may, however, be obtained in the BDCM model. We start by remarking that in the study of low lying excitations of the n-body systems the higher order components of the wave functions, which involve n valence and (2p-2h) core-excitations are poorly admixed in the model space and can be linearized. Within this approximation, the model commutator equations are suitable to be restricted to a finite space. The linearized system of the commutator equations is then solved exactly in terms of the CFT which calculates the n-body matrix elements in an expedite and exact way.

In the following we illustrate the method by considering two valence particles. Following Ref. 2), we calculate the effective Hamiltonian by using only the S_2 correlation operator and obtain

$$\begin{aligned} H_{\text{eff}} &= e^{-iS_2} H e^{iS_2} = \sum_{\alpha\beta} \langle \alpha | t | \beta \rangle a_\alpha^\dagger a_\beta + \sum_{\alpha\beta\gamma\delta} \langle \Psi_{\alpha\beta} | v_{12}^l | \Psi_{\gamma\delta} \rangle a_\alpha^\dagger a_\beta^\dagger a_\delta a_\gamma \\ &= \sum_{\alpha\beta} \langle \alpha | t | \beta \rangle a_\alpha^\dagger a_\beta + \sum_{\alpha\beta\gamma\delta} \langle \Psi_{\alpha\beta} | v | \Psi_{\gamma\delta} \rangle a_\alpha^\dagger a_\beta^\dagger a_\delta a_\gamma, \end{aligned} \tag{2·1}$$

where v_{12}^l is the long component of the two body interaction (note that the v_{12}^l is in the following equations simply denoted as v). The $\Psi_{\alpha\beta}$ is the two particle correlated wave function:

$$\Psi_{\alpha\beta} = e^{iS_2} \Phi_{\alpha\beta}. \tag{2·2}$$

In dealing with complex nuclei, however, the $(S_i,\ i = 3 \cdots n)$ correlations should also be considered.

The evaluation of these diagrams is, due to the exponentially increasing number of terms, difficult in a perturbation theory.

We note, however, that one way to overcome this problem is to work with $e^{i(S_1+S_2+S_3+\cdots+S_i)}$ operator on the Slater determinant by keeping the n-body Hamiltonian uncorrelated.

After having performed the diagonalization of the n-body Hamilton operator we can calculate the form of the effective Hamiltonian which, by now, includes correlation operators of complex order.

We write the two particle states in second quantization by discarding for simplicity the isospin quantum numbers:

$$\Phi_{2p} \longrightarrow A_1^\dagger(\alpha_1 J)|0\rangle = [a_{j_1}^\dagger a_{j_2}^\dagger]_M^J |0\rangle, \tag{2·3}$$

where the operators $a_{j_1}^\dagger a_{j_2}^\dagger$ create two coupled particles in the open shells and we analyze the structure of the particle dynamics, generated by the correlation operator, via the following commutator:

$$[H, A_1^\dagger(\alpha_1 J)]|0\rangle = \left[\left(\sum_\alpha \epsilon_\alpha a_\alpha^\dagger a_\alpha + \frac{1}{2} \sum_{\alpha\beta\gamma\delta} \langle \alpha\beta | v(r) | \gamma\delta \rangle a_\alpha^\dagger a_\beta^\dagger a_\delta a_\gamma \right), (a_{j_1}^\dagger a_{j_2}^\dagger)^J \right] |0\rangle. \tag{2·4}$$

In order to have a compact index definition we have introduced:

$$\alpha_1 \longrightarrow j_1 j_2. \tag{2·5}$$

By using some operator's algebra and by including in the results linear and nonlinear terms we calculate:

$$[H, A_1^\dagger(\alpha_1 J)]|0\rangle = \sum_{\beta_1} \Omega(2p|2p')A_1^\dagger(\beta_1 J)]|0\rangle + \sum_{\beta_2 J_1' J_2'} \Omega(2p|3p1h)A_2^\dagger(\beta_2 J_1' J_2' J)]|0\rangle. \tag{2·6}$$

In Eq. (2·6) the $A_1^\dagger(\beta_1 J)$ operators are those of Eq. (2·3) and the $A_2^\dagger(\beta_2 J_1' J_2' J)$ are defined below:

$$\Phi_{3p1h} \longrightarrow A_2^\dagger(\beta_2 J_1' J_2' J)|0\rangle = ((a_{j_1'}^\dagger a_{j_2'}^\dagger)^{J_1'}(a_{j_3'}^\dagger a_{j_4'})^{J_2'})^J|0\rangle. \tag{2·7}$$

In Eq. (2·7) we have used the additional convention:

$$\beta_2 \longrightarrow j_1' j_2' j_3' j_4' \tag{2·8}$$

and we have associated:

$$\begin{aligned} &J_1' \text{ to the coupling of } j_1' j_2', \\ &J_2' \text{ to the coupling of } j_3' j_4'. \end{aligned} \tag{2·9}$$

Having extended the commutator as in Eq. (2·6), we have also to calculate the commutator equation for the $A_2^\dagger(\alpha_2 J_1 J_2 J)$ operators as given below:

$$\begin{aligned} &[H, A_2^\dagger(\alpha_2 J_1 J_2 J)]|0\rangle \\ &= \sum_{\beta_2 J_1' J_2'} \Omega(3p1h|3p'1h')A_2^\dagger(\beta_2 J_1' J_2' J)|0\rangle + \sum_{\beta_3 J_1' J_2' J_3'} \Omega(3p1h|4p2h)A_3^\dagger(\beta_3 J_1' J_2' J_3' J)|0\rangle, \end{aligned} \tag{2·10}$$

where we have introduced the (4p-2h) wave functions defined below:

$$\Phi_{4p2h} \longrightarrow A_3^\dagger(\beta_3 J_1' J_2' J_3' J)|0\rangle = (((a_{j_1'}^\dagger a_{j_2'}^\dagger)^{J_1'}(a_{j_3'}^\dagger a_{j_4'})^{J_2'})^{J_{12}}(a_{j_5'}^\dagger a_{j_6'})^{J_3'})^J|0\rangle, \tag{2·11}$$

and where we have consistently extended the definition given in Eqs. (2·5) and (2·9):

$$\beta_3 \longrightarrow j_1' j_2' j_3' j_4' j_5' j_6' \tag{2·12}$$

with

$$\begin{aligned} &J_1' \text{ associated to the coupling of } j_1' j_2', \\ &J_2' \text{ associated to the coupling of } j_3' j_4', \\ &J_3' \text{ associated to the coupling of } j_5' j_6'. \end{aligned} \tag{2·13}$$

In the definition of $A_3^\dagger(\beta_3 J_1' J_2' J_3' J)$ the coupling of J_1' to J_2' to J_{12} has been discarded from the notation. In Eqs. (2·6) and (2·10) the Ω are the matrix elements of the Hamilton operator in the model wave functions. The next step would be then the computation of the commutator of the Hamiltonian with the $A_3^\dagger(\beta_3 J_1' J_2' J_3' J)$ operators. Here we linearize these contributions by considering that in the study of the

low energy spectrum and in the calculation of ground-state correlated distributions the $A_3^\dagger(\beta_3 J_1' J_2' J_3' J)$ terms are poorly contributing. The linearization is performed as in Ref. 25) by applying to the (4p2h) terms

$$\sum_{\alpha\beta\gamma\delta} \langle \alpha\beta | v(r) | \gamma\delta \rangle a_\alpha^\dagger a_\beta^\dagger a_\delta a_\gamma A_3^\dagger(\beta_3 J_1' J_2' J_3' J), \tag{2·14}$$

the Wick theorem and to discard the normal order terms. Within this linearization approximation we generate from the commutator equations of Eqs. (2·6) and (2·10) non-perturbative solutions of the EoM, i.e., the eigenvalue equations for the mixed mode system:

$$[H, A_1^\dagger(\alpha_1 J)]|0\rangle = \sum_{\beta_1} \Omega(2p|2p') A_1^\dagger(\beta_1 J)|0\rangle + \sum_{\beta_2 J_1' J_2'} \Omega(2p|3p'1h') A_2^\dagger(\beta_2 J_1' J_2' J)|0\rangle, \tag{2·15}$$

and

$$\begin{aligned}[H, A_2^\dagger(\alpha_2 J_1 J_2 J)]|0\rangle = &\sum_{\beta_1} \Omega(3p1h|2p') A_1^\dagger(\beta_1 J)|0\rangle \\ &+ \sum_{\beta_2 J_1' J_2'} \Omega(3p1h|3p'1h') A_2^\dagger(\beta_2 J_1' J_2')|0\rangle.\end{aligned} \tag{2·16}$$

Within the application of the GLA approximation we convert Eqs. (2·6) and (2·10) in an eigenvalue equation for the configuration mixing wave functions (CMWFs) of the model. In fact, the linearization provides the additional matrix elements necessary to write the following identity:

$$\Omega(3p1h|3p'1h') = \langle j_1 j_2 j_3 j_4 | v(r) | j_1' j_2' j_3' j_4' \rangle, \tag{2·17}$$

and to introduce the off-diagonal matrix elements which couple the (2p) to the (3p1h) subspaces. Now, by writing Eqs. (2·15) and (2·16) in the following matrix form:

$$\begin{aligned}\begin{pmatrix} [H, A_1^\dagger(\alpha_1 J)]|0\rangle \\ [H, A_2^\dagger(\alpha_2 J_1 J_2 J)]|0\rangle \end{pmatrix} = &\begin{pmatrix} E_{2p} + \Omega(2p|2p') & \Omega(2p|3p'1h') \\ \Omega(3p1h|2p') & E_{3p1h} + \Omega(3p1h|3p'1h') \end{pmatrix} \\ &\cdot \begin{pmatrix} A_1^\dagger(\beta_1 J)|0\rangle \\ A_2^\dagger(\beta_2 J_1 J_2 J)|0\rangle \end{pmatrix},\end{aligned} \tag{2·18}$$

and by multiplying to the left with

$$\begin{pmatrix} \langle 0|A_1(\alpha_1 J) \\ \langle 0|A_2(\alpha_2 J_1 J_2 J) \end{pmatrix}, \tag{2·19}$$

we generate the eigenvalue equation for the dressed particles:

$$\begin{aligned}\sum_{\beta_1 \beta_2 J_1' J_2'} &\begin{pmatrix} E_{2p} + \langle A_1(\alpha_1 J)|v(r)|A_1^\dagger(\beta_1 J)\rangle & \langle A_1(\alpha_1 J)|v(r)|A_2^\dagger(\beta_2 J_1' J_2' J)\rangle \\ \langle A_2(\alpha_2 J_1 J_2 J)|v(r)|A_1^\dagger(\beta_1 J)\rangle & E_{3p1h} + \langle A_2(\alpha_2 J_1 J_2 J)|v(r)|A_2^\dagger(\beta_2 J_1' J_2' J)\rangle \end{pmatrix} \\ &\cdot \begin{pmatrix} \chi_1(\beta_1 J) \\ \chi_2(\beta_2 J_1' J_2' J) \end{pmatrix} = E \begin{pmatrix} \chi_1(\alpha_1 J) \\ \chi_2(\alpha_2 J_1 J_2 J) \end{pmatrix} |0\rangle.\end{aligned} \tag{2·20}$$

In Eq. (2·20) $E_{2p} = \epsilon^{HF}_{j_1} + \epsilon^{HF}_{j_2}$ and $E_{3p1h} = \epsilon^{HF}_{j_1} + \epsilon^{HF}_{j_2} + \epsilon^{HF}_{j_3} - \epsilon^{HF}_{j_4}$ are the Hartre-Fock energies (see Appendix C) while the χ are the projections of the model states:

$$|\Phi^J_{2p}\rangle = \chi_1(\alpha_1 J)A_1(\alpha_1 J)|0\rangle + \chi_2(\alpha_2 J_1 J_2 J)A_2(\alpha_2 J_1 J_2 J|0\rangle \tag{2·21}$$

to the basic vectors 2p, 3p1h. To conclude, although the (4p-2h) CMWFs are not active part of the model space, they are important for structure calculations. One may therefore associate the GLA approximation to a parameter which describes the degree of complexity of the model CMWFs (the method used to define the CMWFs is given in Appendices A–C). Within the first order linearization we obtain the EoM for the shell model while within the second and third order linearization approximations we derive the EoM of valence particles coexisting with the complex particle-hole structure of the excited states.

In this paper we solve Eq. (2·20) self-consistently (see Appendix D). The solutions for the first iteration step are obtained by diagonalizing the eigenvalue equation (2·20). The first step of the iterative method generates the dynamic amplitudes for the two dressed particles, i.e. two particles coexisting with the 3p1h structures. With the calculated eigenvectors we recompute then the matrix elements $\langle j_1 j_2|v(r)|j_1 j_2 j_3 j_4\rangle$ and $\langle j_1 j_2 j_3 j_4|v(r)|j'_1 j'_2 j'_3 j'_4\rangle$ and we diagonalize again the eigenvalue equation. The iterations are repeated until the stabilization of the energies has been reached.

To be noted that since we are working in coupled particle-particle and particle-hole bases we need both particle-particle and particle-hole matrix elements (these terms where set to zero in the original work of Brückner[4)]) in orders to diagonalize the eigenvalue equation. The calculation of these matrix elements is, however, complicated by the number of terms which have to be evaluated in order to solve the introduced iterative equations. As in Ref. 3) one solves this problem by using the cluster factorization theory CFT which provides a quick and exact numerical method to perform the calculations of the matrix elements. The starting point of the CFT theory is to expand the CMWFs base introduced for (3p1h) states in terms of cluster factorization coefficients (CFC) denoted in the following U and V:

$$\begin{aligned}
&|3p1h\rangle^J = A^\dagger_2(\alpha_2 J_1 J_2 J)|0\rangle \\
&= \sum_{J_r J_s \epsilon_i} {}^5V^{(3,1)}_J(\alpha_2 J_1 J_2|\}\epsilon_i J_r \bar{\epsilon}_i J_s)|[A^\dagger_1(\epsilon_i J_r)B^\dagger_1(\bar{\epsilon}_i J_s)]^J|0\rangle \\
&+ \sum_{J_r J_s \alpha_j} {}^5U^{(3,1)}_J(\alpha_2 J_1 J_2|\}\alpha_j J_r \bar{\alpha}_j J_s)|[B^\dagger(\alpha_j J_r)A^\dagger_1(\bar{\alpha}_j J_s)]^J|0\rangle \\
&= \sum_{J_r J_s \epsilon_i} {}^5V^{(3,1)}_J(\alpha_2 J_1 J_2|\}\epsilon_i J_r \bar{\epsilon}_i J_s)|[\epsilon_i J_r \bar{\epsilon}_i J_s]^J|0\rangle \\
&+ \sum_{J_r J_s \alpha_j} {}^5U^{(3,1)}_J(\alpha_2 J_1 J_2|\}\alpha_j J_r \bar{\alpha}_j J_s)|[\alpha_j J_r \bar{\alpha}_j J_s]^J|0\rangle,
\end{aligned} \tag{2·22}$$

where the (α_2) coordinates of the (3p1h) model states have been expanded in terms of active (passive) particle-particle and passive (active) particle-hole coordinates as

given below:

$$\alpha_2 \rightarrow \epsilon_i(J_r)(\text{active particle-particle})\bar{\epsilon}_i(J_s)(\text{passive particle-hole}) \\ +\alpha_j(J_r)(\text{active particle-hole})\bar{\alpha}_j(J_s)(\text{passive particle-particle}). \tag{2·23}$$

In Eq. (2·22) the superscript on the left of the V and U indicates the total number of pairs (2(two pairs) + 1 = 5) while the superscripts on the right the number of particles and holes. There we have also introduced the creation operators of a particle-hole pair:

$$(ph) \longrightarrow B_1^\dagger(\alpha_1 J)|0\rangle = [a_{j_1}^\dagger a_{j_2}]_M^J|0\rangle \tag{2·24}$$

and postulated that the sum over (i) is to be extended over the six combinations (partitions) of particle-particle pairs formed by the (3p1h) model space and (j) over the three combinations of particle-hole pairs:

$$\begin{array}{lll} \alpha_2 \rightarrow & \epsilon_i\bar{\epsilon}_i & \alpha_j\bar{\alpha}_j \\ j_1j_2j_3j_4^{-1} \rightarrow & (j_ij_j)(j_kj_4^{-1}) & (j_kj_4^{-1})(j_ij_j) \end{array}. \tag{2·25}$$

Within this convention we reproduce exactly the the (3p1h) CMWFs. In Eq. (2·22) the sum over $(\bar{\alpha}_i)$ and $(\bar{\epsilon}_i)$ has not been given explicitly because these indices are complementary to the (α_i) and (ϵ_i) in the sense of Eq. (2·25). The sum over J_r and J_s take care of the fact that by calculating the (3p1h) matrix elements in the traditional way, the coupling of the j of the (2p) is not the same as in the coupling postulated for (3p1h) wave functions. The definitions of active and passive components separate the matrix elements of the interaction in particle-particle and particle-hole matrix elements.

It has to be remarked that, due to the used iterative method, the final results are almost independent from the initial choice of the interaction because after the first iteration the two body potential is modified by the contributions of both types of matrix elements.

Matrix elements calculated by using the first term of Eq. (2·22) are related to the Brückner theory,[4] while those evaluated with the second term have been considered in the folded diagram theory of Kuo.[5]

In order to calculate the CFC-${}^5V_J^{(3,1)}(\alpha_2 J_1 J_2|\}\epsilon_i J_r \bar{\epsilon}_i J_s)$ we introduce[3] the following operator:

$$\pi_{m_k}^k(2) = [(a_{i'}^\dagger a_i^\dagger)^{J_i}(a_j a_{j'})^{J_i'}]_{m_k}^k \tag{2·26}$$

which destroys and creates a particle pair and we evaluate his effect on the 3p1h wave function. In Eq. (2·22) the two in the parenthesis indicate that the operators are working on the space spanned by two boson (two pairs). We calculate

$$\pi_{m_k}^k(2)A_2^\dagger(\alpha_2 J_1 J_2 JM)|0\rangle = C^{JkJ}_{Mm_kM'}(\text{Coef}_1 \cdot ([a_{i'}^\dagger a_i^\dagger]^{J_r}[a_{j_3}^\dagger a_{j_4}]^{J_s})_{M'}^J \\ +\text{Coef}_2 \cdot ([a_i^\dagger a_{j_2}^\dagger]^{J_r}[a_{i'}^\dagger a_{j_4}]^{J_s})_{M'}^J + \text{Coef}_3 \cdot ([a_{j_1}^\dagger a_i^\dagger]^{J_r}[a_{i'}^\dagger a_{j_4}]^{J_s})_{M'}^J)|0\rangle. \tag{2·27}$$

The $\text{Coef}_{\lambda_i}, \lambda_i = 1, 2, 3$ are given in Appendix E. By multiplying Eq. (2·27) to the left with $\langle 0|A_2(\alpha_2 J_1 J_2)$ we obtain the following equation:

$$\frac{\langle 0|A_2(\alpha_2 J_1 J_2 JM)\pi_{m_k}^k(2)A_2^\dagger(\alpha_2 J_1 J_2 JM)|0\rangle}{(\text{Coef}_1 + \text{Coef}_2 + \text{Coef}_3)} = C^{JkJ}_{Mm_kM'}, \tag{2·28}$$

where we have introduced the Clebsch-Gordan coefficients $C^{JkJ}_{Mm_kM'}$. Equation (2·28) defines the matrix elements of a unitary operator, i.e., by applying the unitary operator $\frac{\pi^k_{m_k}(2)}{\mathrm{Coef}_1+\mathrm{Coef}_2+\mathrm{Coef}_3}$ on the left of a wave function of the type $|3\mathrm{p}1\mathrm{h}\rangle^J_M$ we reproduce the same wave function in a rotated frame. It follows that the structure defined by Eq. (2·28) is that of a full linear group in $(2J+1)$ dimension and of its unitary subgroup U_{2J+1}. The calculation of the transformation coefficients is now reduced to the construction of the $\mathrm{Coef}_{\lambda_i}$ coefficients. In order to demonstrate this, let us now operate with the Casimir operator of the group $(\pi^k_{m_k}(2)\otimes(\pi^k_{m_k}(2))^\dagger)^0_0$ on the left-hand side of Eq. (2·22). We obtain

$$\langle A_2(\alpha_2 J_1 J_2 J)\|(\pi^k_{m_k}(2)\otimes(\pi^k_{m_k}(2))^\dagger)^0_0\|A^\dagger_2(\alpha_2 J_1 J_2 J)\rangle = \sum_{\lambda_i\lambda_j}\mathrm{Coef}_{\lambda_i}\mathrm{Coef}_{\lambda_j}, \quad (2\cdot29)$$

where the double bar matrix elements have been introduced because the CFC are independent from the m quantum numbers and where the subscript λ_i classifies the three different partitions spanned by the particles in the (3p1h) wave functions. On the other hand, considering that

$$(\pi^k_{m_k}(2)\otimes(\pi^k_{m_k}(2))^\dagger)^0_0 = \sum_{i=1}^{\lambda_i}(\pi^k_{m_k}(1,i)\pi^0_0(\bar{1},i)\otimes((\pi^0_0(\bar{1},i))^\dagger(\pi^k_{m_k}(1,i))^\dagger)^0_0, \quad (2\cdot30)$$

where the sum is running over all the possible partitions, we calculate by using Eq. (2·22):

$$\begin{aligned}&\langle A_2(\alpha_2 J_1 J_2 J)||(\pi^k_{m_k}(1,i)\pi^0_0(\bar{1},i)\otimes((\pi^0_0(\bar{1},i))^\dagger(\pi^k_{m_k}(1,i))^\dagger)^0_0||A^\dagger_2(\alpha_2 J_1 J_2 J)\rangle\\ &= {}^5V^{\dagger(3,1)}_J(\alpha_2 J_1|\}\lambda_i\epsilon_i J_r\bar{\epsilon}_i J_s)\,{}^5V^{(3,1)}_J(\alpha_2 J_1|\}\lambda_i\epsilon_i J_r\bar{\epsilon}_i J_s). \quad (2\cdot31)\end{aligned}$$

In Eq. (2·31) we have introduced the unit operators $\pi^0_0(\bar{1},i)$ defined by

$$\langle B_1(\bar{\epsilon}_j J'_s)|(\pi^0_0(\bar{1},i))^\dagger\pi^0_0(\bar{1},i)|B^\dagger_1(\bar{\epsilon}_i J_s)\rangle = \delta_{\bar{\epsilon}_i\bar{\epsilon}_j}\delta_{J_sJ'_s}. \quad (2\cdot32)$$

By equating Eqs. (2·29) and (2·31) we obtain

$${}^5V^{\dagger(3,1)}_J(\alpha_2 J_1|\}\lambda_i\epsilon_i J_r\bar{\epsilon}_i J_s)\,{}^5V^{(3,1)}_J(\alpha_2 J_1|\}\lambda_i\epsilon_i J_r\bar{\epsilon}_i J_s) = \sum_{\lambda_i\lambda_j}\mathrm{Coef}_{\lambda_i}\mathrm{Coef}_{\lambda_j}. \quad (2\cdot33)$$

Equation (2·33) is given in matrix form in Appendix E. Note that from the diagonalization of Eq. (E·4) we derive the square of the CFC. In order to calculate the CFC we introduce the same phase convention used to define the Clebsch-Gordan coefficients. Analogously also for the operator

$$u^k_{m_k}(2) = [(a^\dagger_i a_j)^{J_i}(a^\dagger_{j'}a_{i'})^{J'_i}]^k_{m_k} \quad (2\cdot34)$$

which destroys and creates a particle-hole pair. The normalization factors for these operators $(c_{\mu_i}; i = 4,5,6)$ are given in Appendix D. A numerical example for the calculation of these coefficients is given in Appendix F. By using Eq. (E·4) and the

evaluated CFC, we can now calculate the matrix elements of the nuclear interaction in the (3p1h) CMWFs. We derive

$$\begin{aligned}
&\langle 3p1h|v(r)|3p'1h'\rangle = \langle A_2(\alpha_2 J_1 J_2 J)|v(r)|A^\dagger(\beta_2 J_1' J_2' J)\rangle \\
&= \sum_{\lambda_i\lambda_j\epsilon_i\epsilon_j J_r J_s J_r' J_s'} {}^5V_J^\dagger(\alpha_2 J_1 J_2|\}\lambda_i\epsilon_i J_r\bar{\epsilon}_i J_s)\,{}^5V_J(\beta_2 J_1' J_2'|\}\lambda_j\epsilon_j J_r'\bar{\epsilon}_j J_s') \\
&\langle[\lambda_i\epsilon_i J_r\bar{\epsilon}_i J_s]^J|v(r)|[\lambda_j\epsilon_j J_r'\bar{\epsilon}_j J_s']^J\rangle \\
&+ \sum_{\mu_i\mu_j\alpha_i\alpha_j J_r J_s J_r' J_s'} {}^5U_J^\dagger(\alpha_2 J_1 J_2|\}\mu_i\alpha_i J_r\bar{\alpha}_i J_s)\,{}^5U_J(\beta_2 J_1' J_2'|\}\mu_j\alpha_j J_r'\bar{\alpha}_j J_s') \\
&\langle[\mu_i\alpha_i J_r\bar{\alpha}_i J_s]^J|v(r)|[\mu_j\alpha_j J_r'\bar{\alpha}_j J_s']^J\rangle \\
&= \sum_{\lambda_i\lambda_j\epsilon_i\epsilon_j J_r J_r' J_s} {}^5V_J^\dagger(\alpha_2 J_1 J_2|\}\lambda_i\epsilon_i J_r\bar{\epsilon}_i J_s)\,{}^5V_J(\beta_2 J_1' J_2'|\}\lambda_j\epsilon_j J_r'\bar{\epsilon}_j J_s) \\
&\langle\lambda_i\epsilon_i|v(r)|\lambda_j\epsilon_j\rangle_a^{J_r} \\
&+ \sum_{\mu_i\mu_j\alpha_i\alpha_j J_r J_r' J_s} {}^5U_J^\dagger(\alpha_2 J_1 J_2|\}\mu_i\alpha_i J_r\bar{\alpha}_i J_s)\,{}^5U_J(\beta_2 J_1' J_2'|\}\mu_j\alpha_j J_r'\bar{\alpha}_j J_s) \\
&\langle\mu_i\alpha_i|v(r)|\mu_j\alpha_j\rangle_a^{J_r}. \qquad (2\cdot35)
\end{aligned}$$

In Eq. (2·35) we have two types of matrix elements, the particle-particle matrix elements which, by choosing one λ_i and μ_i partitions, can be written as

$$\langle\lambda_1\epsilon_1|v(r)|\lambda_1\epsilon_1'\rangle_a^{J_r} = \langle j_1 j_2|v(r)|j_1' j_2'\rangle_a^{J_r}, \qquad (2\cdot36)$$

and the particle-hole matrix elements:

$$\langle\mu_1\alpha_1|v(r)|\mu_1\alpha_1'\rangle_a^{J_r} = \langle j_3 j_4|v(r)|j_3 j_4\rangle_a^{J_r}. \qquad (2\cdot37)$$

The matrix elements of Eq. (2·37) which generate the interaction with the core clusters are not considered by the microscopic calculation of Refs. 6) and 9) where the effective Hamiltonian is obtained by summing only over ladder diagrams.[4] By using the diagonal matrix elements of Eq. (2·35) and the off-diagonal matrix elements given in Ref. 3) we diagonalize Eq. (2·20) and obtain the amplitudes $\chi(\alpha_1)$ and $\chi(\alpha_2)$ of the mixed modes (2p) and (3p1h). The calculation of the ground and excited state distributions and of the magnetic moments is then performed in terms of these amplitudes. The formula of the correlated distribution for the ground state of even nuclei is given in Appendix H.

§3. Results

In order to perform structure calculations, we have to define a single-particle base with the relative "single-particle energies" and to choose the nuclear two body interactions. The single-particle energies of these levels are taken from the known experimental level spectra of the neighboring nuclei[27] (see Appendix C) and given in Table I. For the experimentally unknown single-particle energies of the fp shells we use the corresponding energies for the mass A-9 nuclei scaled according to the different binding energies. Our single-particle energies agree reasonably well with those calculated in Ref. 28). Some of these levels are not bound. In this paper we

perform as in Ref. 9) calculations by assuming all levels as bound. It has to be remembered, however, that the energies of Table I are used only in the first stage of the iteration procedure explained in Appendix F.

For the particle-particle interaction, we use the G-matrix obtained from Yale potential.[29] These matrix elements are evaluated by applying the e^S correlation operator, truncated at the second order term of the expansion, to the harmonic oscillator base with size parameter $b = 1.76$ fm. This value is consistent with the value used by Kuo.[30] As elucidate in Ref. 3) the potential used by the BDCM is separated in low and high momentum components. Therefore, the effective model matrix elements calculated within the present separation method and those calculated by Kuo[31] are pretty similar. The separation method generates matrix elements which are almost independent from the radial shape of the different potentials generally used in structure calculations.

The particle-hole matrix elements could be calculated from the particle-particle matrix elements via a re-coupling transformation. We prefer to use the phenomenological potential of Ref. 24). The same size parameter as for the particle-particle matrix elements has been used.

One can generate the center-of-mass (CM) spurious states according to Refs. 32) and 33), and evaluate the overlap between these states and the nuclear eigenstates of the model (see Appendix B). Model components having with the corresponding CM components an overlap greater than 10% were treated as spurious states and discarded. This is a convenient approximation considering that in our model space the energy of the CM is varying between 18 and 20 MeV.

By using a base formed by 9 (2p) and 112 3p1h-states we calculate the distribution of the ground state of ^{6}He given in Fig. 1. The spectroscopic factor for the ground state wave function, defined in Appendix G, and the most significant components of the ground state wave function are given in Table IX. In Fig. 1 we plot three distributions: 1) the correlated charge distribution of ^{6}He calculated with Eq. (F·6), 2) the correlated charge distribution of ^{6}He calculated with Eq. (F·6) but neglecting the folded diagrams, 3) the charge distribution calculated for two correlated protons in the $1s_{\frac{1}{2}}$ shell. A charge radius of 2.25 fm has been obtained for the distribution a), a radius of 2.39 fm for the distribution b), and a radius of 2.09 fm for the distribution c).

In Table II the calculated charge radii are compared with the radii calculated by the other theoretical models and with the radius obtained by the IS theory. The radius calculated with the distribution c) (single-particle) is in agreement with the radius obtained by the IS theory and with those of the other theoretical models. The BDCM increases, however, the charge radius of ^{6}He. One reason for this slightly disagreement can rely on the effect of the correlation operator which is neglected either in the evaluation of the charge radii via the IS theory or in the other theoretical model calculations. As shown in Ref. 3) the correlations are also important in the analysis of the matter radius of ^{6}He. Here the larger matter radius reproduces reasonable well the proton elastic scattering cross section measured at GSI at 717 MeV/u calculated by using the Glauber method in the whole range of data.[35]

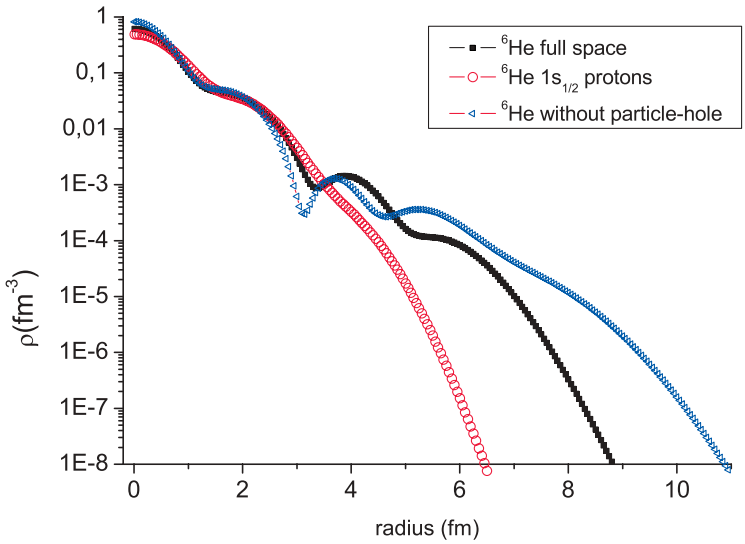

Fig. 1. Calculated charge distributions of ^{6}He: black — calculated with a full configuration mixed base, blue — calculated without the particle-hole diagrams, and red — calculated for two protons in the $s_{\frac{1}{2}}$ shell.

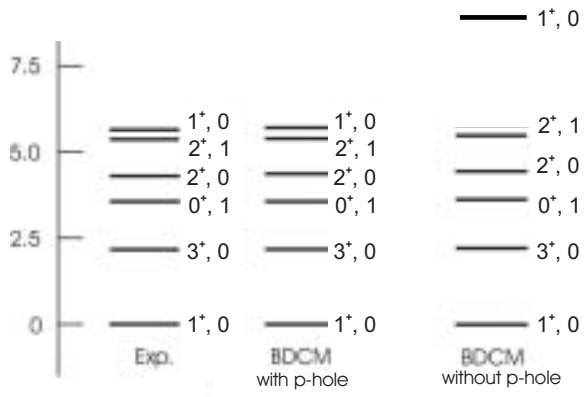

Fig. 2. Calculated spectrum of ^{6}Li: Left: energy levels calculated by allowing the excitation of the $1s_{\frac{1}{2}}$- and the $1p_{\frac{3}{2}}$-hole. Right: energy levels calculated by restricting the hole to the $1s_{\frac{1}{2}}$.

The energy of the low lying spectrum of ^{6}Li is calculated by defining a coupled base in which a proton-neutron pair in the (*psd*) single-particle scheme of Table I are interacting with the (3p1h) states generated by exciting the hole from the lowest (1*s*) shell. Within the model dimension of 13 (2p) and 196 (3p1h) components we define the ground state wave functions. The spectroscopic factor for the ground state

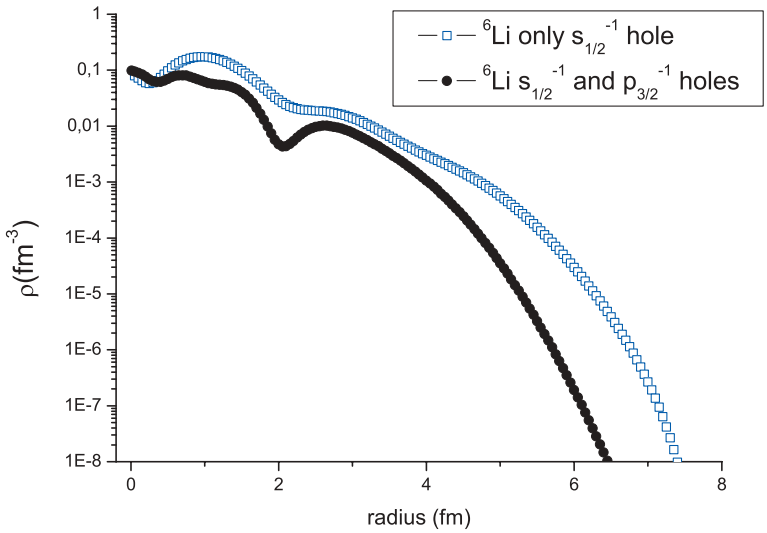

Fig. 3. Calculated charge distributions of ^{6}Li: blue — calculated by restricting the hole to the $s_{\frac{1}{2}}$-state; black — calculated by considering $s_{\frac{1}{2}}$- and $p_{\frac{1}{2}}$-hole. The configuration space considered is formed by 13 two particle (shell model)-states and 512-(3p1h) states.

of ^{6}Li and the most significant components of the ground state wave function are given in Table X. By using this model space we obtain the spectrum shown on the right-hand side of Fig. 2. For the ground state this model space is, however, not large enough to reproduce the second 1^+ level and the magnetic moment of the ground state.[36)] The magnetic moment of the ground state calculated in this model space is 0.875 nm therefore larger than the experimental value (0.822 nm). The second spectrum is calculated introducing for the ground state a much larger space with dimension of 525 components (13 two particle shell model states and 512 (3p1h) states) which includes also the excitation of the particles from the $1p_{\frac{3}{2}}$ state. Within this dimensional space the spectroscopic factor for the ground state of ^{6}Li, defined in Appendix G, and the most significant components are given in Table XI. Within this space we reproduce also the energy of the second 1^+ level given on the left-hand side of Fig. 2. To be considered that in other theoretical models the 1^+ always lies at an energy that is too high. Since we plot the spectrum relative to the ground state energy, the effect of enlarging the base also for the other states is negligible at least for the first plotted 2^+ and 3^+ levels. The magnetic moment of the ground state calculated for the large model space is 0.821 nm. The value is in good agreement with the experimental value. The charge distributions calculated within these two model spaces are given in Fig. 3. The two distributions are labeled: 1) charge distribution calculated for the small configuration space and 2) charge distribution calculated for the large space. The calculated charge radii are respectively $\langle r^2_{ch}\rangle^{\frac{1}{2}}$ equal to 2.627 fm for the small model space and to 2.55 fm for the large space. Both values reproduce

well the charge radius of 2.55 fm obtained in Ref. 17) from the electron scattering experiments. Calculation of the electric scattering form factor measured in Ref. 17) for both charge distributions is presently under consideration.

§4. Conclusions

In this paper we have investigated the effect of the microscopic correlation operators on the spectra and the charge distributions of ^{6}He and ^{6}Li. The microscopic correlation has been separated in short- and long-range correlations according the definition of Shakin.[2)] The short-range correlation has been used to define the effective Hamiltonian of the model while the long-range is used to calculate the structures and the distributions of exotic nuclei. As given in the work of Shakin, only the two body short-range correlation needs to be considered in order to derive the effective Hamiltonian especially if the correlation is of very short range. For the long-range correlation operator, however, the "three body component" of the correlation operator is important and should not be neglected. The effect of the "three body correlation operator" is to introduce in the theory a three body interaction. Therefore the use of the genuine three body interaction of the other theoretical model could, in the present theory, generate double counting of diagrams.

By using generalized linearization approximations and cluster factorization coefficients we can perform expedite and exact calculations for the structure of ^{6}He and ^{6}Li. Very good results for the spectrum of ^{6}Li have been obtained by considering large configuration spaces. Within correlated distributions we obtain charge radii slightly larger than those calculated within either non-correlated distributions or IS experiments.

This result should serve as motivation to a reevaluation of the different terms of the IS theory, i.e. the MS, which is mainly calculated in a perturbative approximation, and the FS, which is generally calculated in a point nucleus approximation, should be reevaluated within the non-perturbative BDCM.

Appendix A

—— Definition of the Model CMWFs ——

In the BDCM the degree of linearization applied to the commutator equations defines the CMWFs of the model. For $A = 6$ the model space is formed by two valence particle states and by the full set of the (3p1h) CMWFs. These different components are associated to the following linearization mechanism: a) In the zero order linearization approximation we retain only two particle states:

$$\Psi^{2p}(j_1 j_2 J) = [a^\dagger_{j_1} a^\dagger_{j_2}]^{JM}|0\rangle. \tag{A·1}$$

For the two particles we distinguish between
1) effective valence space which is used to diagonalize the EoM,
2) complementary high excited single-particle states which are used to compute the G-matrix.
b) In the first order linearization approximation we include in the dynamic theory

also the (3p1h) terms. These are generated by the application of the correlation operator of the third order to the particles in the open shell states. Within this linearization approximation the CMWFs of the model are defined by

$$\Psi^{\rm dressed}(j_1 j_2 J) = ([a^\dagger_{j_1} a^\dagger_{j_2}] + [a^\dagger_{j_1} a^\dagger_{j_2}]^{J_{12}} [a^\dagger_{j_3} a_{j_4}]^{J_{34}})^{JM} |0\rangle. \tag{A·2}$$

The (3p1h) CMWFs are then expanded according to Eq. (2·22). This expansion allows to orthogonalize the CMWFs in an easy way. c) The (4p2h) states which characterize the second order linearization step are not included in the model space but, linearized, generate the eigenvalue equation of the model (2p)+(3p1h) states.

Appendix B
—— *Center of Mass Correction* ——

Before performing the diagonalization of relative Hamilton operator in the CMWFs defined in Appendix A we have to eliminate the spurious center of mass states. We start to compute, following the calculations of Refs. 32) and 33), the percent weights of spurious states in the model wave functions. These can be obtained by calculating the energy of the center of mass according to the following equation:

$$\begin{aligned} E_R &= \int dR \Psi^{\dagger \rm dressed}(j_i j_j J)(R^2) \Psi^{\rm dressed}(j_i j_j J) \\ &+ 2 \sum_{ij} \int d\vec{r_i} d\vec{r_j} \Psi^{\dagger \rm dressed}(j_i j_j J)(\vec{r_i} \cdot \vec{r_j}) \Psi^{\rm dressed}(j'_i j'_j J). \end{aligned} \tag{B·1}$$

In Eq. (B·1) the calculation of the integrals can be performed by using the expansion for the (3p1h) states given in Eq. (2·22) and by considering that for two particle states we have

$$\begin{aligned} &\langle j_i j_j J | (\vec{r_i} \cdot \vec{r_j}) | j_i j_j J \rangle \\ &= \tfrac{4\pi}{3} [\hat{j_i} \hat{j_j}] \begin{pmatrix} j_i & 1 & j_j \\ -\frac{1}{2} & 0 & \frac{1}{2} \end{pmatrix}^2 \begin{Bmatrix} j_i & j_j & J \\ j_i & j_j & 1 \end{Bmatrix} \langle l_i | r | l_j \rangle^2, \end{aligned} \tag{B·2}$$

where

$$\hat{j} = (2j+1). \tag{B·3}$$

By diagonalizing the above operator in the model space we obtain the energy of the center of mass. The overlap with the model space give the degree of "spuriosity" of the different components.

Appendix C
—— *The Single-Particle Energies* ——

The model space which characterize the BDCM is formed by adding even particle to a closed-shell nucleus. The closed shell configuration can be described by a single Slater determinant and one can use the Hartree-Fock theory to obtain the binding energy and the single-particle energies. Alternatively one can remark that for a closed shell nucleus (Z, N) the single-particle energies for the states above the Fermi

surface are related to the binding energies differences:

$$\epsilon_p^{>} = BE(Z,N) - BE^*(Z+1,N) \tag{C·1}$$

and

$$\epsilon_n^{>} = BE(Z,N) - BE^*(Z,N+1). \tag{C·2}$$

The single-particle energies for the states below the Fermi surface are given by

$$\epsilon_p^{<} = BE^*(Z-1,N) - BE(Z,N) \tag{C·3}$$

and

$$\epsilon_n^{<} = BE^*(Z,N-1) - BE(Z,N). \tag{C·4}$$

The BE are ground states binding energies which are taken as positive values, and will be negative for bound states. ($BE^* = BE - E_x$) is the ground state binding energy minus the excitation energy of the excited states associated with the single-particle states. Within this method, which recently has been reintroduced by Brown,[37] we derive the single-particle energies from the known spectra of neighbor nuclei (see Table I).

Table I. Single-particle scheme and single-particle energies (MeV) used to form the model CMWFs.

hole	$1s_{1/2}$							
energy	-20.58							
hole/particle	$1p_{3/2}$							
energy	1.43							
particle	$1p_{1/2}$	$1d_{5/2}$	$2s_{1/2}$	$1d_{3/2}$	$1f_{7/2}$	$2p_{3/2}$	$1f_{5/2}$	$2p_{1/2}$
energy	1.73	17.21	22.23	23.69	25.23	27.18	28.33	29.67

Table II. Calculated charge radii for ^{6}He in fm compared with the results obtained in other theoretical models and with the radius derived within the IS theory.

charge radius of ^{6}He	Model
1.944[34]	no-core shell model
2.09[9]	quantum Monte Carlo technique
2.25 this work	BDCM
2.39 this work	BDCM without the folded diagrams
2.06 this work	two correlated $1s_{\frac{1}{2}}$-protons
1.99[11]	Cluster
1.99[12]	Cluster
1.99[13]	Cluster
$2.054 \pm .014$[10]	Isotopic Shift (Exp.)

Appendix D

—— Iteration Procedure to Calculate Dressed Eigenstates ——

Let us suppose we have two particles in the *sd* shell model states interacting via the (3p1h) CMWFs. The configuration mixed wave functions are

$$\begin{aligned}\Psi_{2p}^{\text{dressed}} &= [a^\dagger_{1d_{\frac{5}{2}}} a^\dagger_{2s_{\frac{1}{2}}}]^2 + [a^\dagger_{1d_{\frac{3}{2}}} a^\dagger_{2s_{\frac{1}{2}}}]^2 \\ &+ \left[[a^\dagger_{1d_{\frac{5}{2}}} a^\dagger_{2s_{\frac{1}{2}}}]^3 [a^\dagger_{2s_{\frac{1}{2}}} a_{1s_{\frac{1}{2}}}]^1\right]^2 + \left[[a^\dagger_{1d_{\frac{3}{2}}} a^\dagger_{2s_{\frac{1}{2}}}]^2 [a^\dagger_{1d_{\frac{5}{2}}} a_{1s_{\frac{1}{2}}}]^3\right]^2 \\ &= \psi_1 + \psi_2 + \psi_3 + \psi_4. \end{aligned} \tag{D·1}$$

This is a solution of the eigenvalue matrix:

$$\begin{pmatrix} E_1 + \langle\psi_1|v(r)|\psi_1\rangle & \langle\psi_1|v(r)|\psi_2\rangle & \langle\psi_1|v(r)|\psi_3\rangle & \langle\psi_1|v(r)|\psi_4\rangle \\ \langle\psi_2|v(r)|\psi_1\rangle & E_2 + \langle\psi_2|v(r)|\psi_2\rangle & \langle\psi_2|v(r)|\psi_3\rangle & \langle\psi_2|v(r)|\psi_4\rangle \\ \langle\psi_3|v(r)|\psi_1\rangle & \langle\psi_3|v(r)|\psi_2\rangle & E_3 + \langle\psi_3|v(r)|\psi_3\rangle & \langle\psi_1|v(r)|\psi_4\rangle \\ \langle\psi_4|v(r)|\psi_1\rangle & \langle\psi_4|v(r)|\psi_2\rangle & \langle\psi_4|v(r)|\psi_3\rangle & E_4 + \langle\psi_4|v(r)|\psi_4\rangle \end{pmatrix} \cdot \begin{pmatrix} \psi_1|0\rangle \\ \psi_2|0\rangle \\ \psi_3|0\rangle \\ \psi_4|0\rangle \end{pmatrix} = 0. \tag{D·2}$$

By diagonalizing the matrix of Eq. (D·2) we obtain four eigenvalues $\tilde{E_1}, \tilde{E_2}, \tilde{E_3}$ and $\tilde{E_4}$, and the four eigenvectors given below:

$$\tilde{\Psi_1} = \chi_1^1|\psi_1\rangle + \chi_2^1|\psi_2\rangle + \chi_3^1|\psi_3\rangle + \chi_4^1|\psi_4\rangle, \tag{D·3}$$

$$\tilde{\Psi_2} = \chi_1^2|\psi_1\rangle + \chi_2^2|\psi_2\rangle + \chi_3^2|\psi_3\rangle + \chi_4^2|\psi_4\rangle, \tag{D·4}$$

$$\tilde{\Psi_3} = \chi_1^3|\psi_1\rangle + \chi_2^3|\psi_2\rangle + \chi_3^3|\psi_3\rangle + \chi_4^3|\psi_4\rangle, \tag{D·5}$$

$$\tilde{\Psi_4} = \chi_1^4|\psi_1\rangle + \chi_2^4|\psi_2\rangle + \chi_3^4|\psi_3\rangle + \chi_4^4|\psi_4\rangle. \tag{D·6}$$

This eigenvalues and eigenvectors are then used to diagonalize the eigenvalue matrix in the second iteration step:

$$\begin{pmatrix} \tilde{E_1} + \langle\tilde{\Psi_1}|v(r)|\tilde{\Psi_1}\rangle & \langle\tilde{\Psi_1}|v(r)|\tilde{\Psi_2}\rangle & \langle\tilde{\Psi_1}|v(r)|\tilde{\Psi_3}\rangle & \langle\tilde{\Psi_1}|v(r)|\tilde{\Psi_4}\rangle \\ \langle\tilde{\Psi_2}|v(r)|\tilde{\Psi_1}\rangle & \tilde{E_2} + \langle\tilde{\Psi_2}|v(r)|\tilde{\Psi_2}\rangle & \langle\tilde{\Psi_2}|v(r)|\tilde{\Psi_3}\rangle & \langle\tilde{\Psi_2}|v(r)|\tilde{\Psi_4}\rangle \\ \langle\tilde{\Psi_3}|v(r)|\tilde{\Psi_1}\rangle & \langle\tilde{\Psi_3}|v(r)|\tilde{\Psi_2}\rangle & \tilde{E_3} + \langle\tilde{\Psi_3}|v(r)|\tilde{\Psi_3}\rangle & \langle\tilde{\Psi_3}|v(r)|\tilde{\Psi_4}\rangle \\ \langle\tilde{\Psi_4}|v(r)|\tilde{\Psi_1}\rangle & \langle\tilde{\Psi_4}|v(r)|\tilde{\Psi_2}\rangle & \langle\tilde{\Psi_4}|v(r)|\tilde{\Psi_3}\rangle & \tilde{E_4} + \langle\tilde{\Psi_4}|v(r)|\tilde{\Psi_4}\rangle \end{pmatrix} = 0, \tag{D·7}$$

where

$$\begin{aligned} &\langle\tilde{\Psi_1}|v(r)|\tilde{\Psi_1}\rangle \\ &= (\chi_1^1)^2\langle\psi_1|v(r)|\psi_1\rangle + (\chi_2^1)^2\langle\psi_2|v(r)|\psi_2\rangle + (\chi_3^1)^2\langle\psi_2|v(r)|\psi_2\rangle + (\chi_4^1)^2\langle\psi_4|v(r)|\psi_4\rangle \\ &+2\chi_1^1\chi_2^1\langle\psi_1|v(r)|\psi_2\rangle + 2\chi_1^1\chi_3^1\langle\psi_1|v(r)|\psi_3\rangle + 2\chi_1^1\chi_4^1\langle\psi_1|v(r)|\psi_4\rangle \\ &+2\chi_2^1\chi_3^1\langle\psi_2|v(r)|\psi_3\rangle + 2\chi_2^1\chi_4^1\langle\psi_2|v(r)|\psi_4\rangle + 2\chi_3^1\chi_4^1\langle\psi_3|v(r)|\psi_4\rangle, \end{aligned} \tag{D·8}$$

where the χ_j^i are the projections of the truncated model space on the basic vectors 2p, 3p1h. The procedure is re-iterated until the energy convergence has been obtained.

Appendix E

—— Basic Equations for the CFT of the (3p1h) CMWFs ——

The normalization factors for the π operators are calculated by using the recoupling algebra of Ref. 26). We obtain

$$\mathrm{Coef}_1=\sum_{kJ'_rJ_r}\sqrt{[\hat{k}\hat{J}]}(-1)^{i+i'+k+J_2+J+1}\left\{\begin{array}{ccc} J_r & k & J_1 \\ J & J_2 & J'_r \end{array}\right\}(1-\delta_{j'2}\delta_{j1}(-1)^{j_1+j_2-J_i})\delta_{J_sJ_2}, \tag{E·1}$$

$$\mathrm{Coef}_2=\sum_{kJ'_rJ^1_rJ^4_rJ_iJ_rJ_s}(\hat{J}'_r\hat{J}^4_r)\sqrt{[\hat{J}_1\hat{J}_2\hat{J}_i\hat{J}^1_r\hat{J}_s\hat{J}^4_r\hat{k}\hat{J}]}(-1)^{i'+J'_r+J^1_r+J_r+J+1}$$
$$\left\{\begin{array}{ccc} j_1 & j_2 & J_1 \\ J & J_2 & J'_r \end{array}\right\}\left\{\begin{array}{ccc} j_3 & j_4 & J_2 \\ J'_r & j_1 & J^1_r \end{array}\right\}\left\{\begin{array}{ccc} i & J^4_r & J'_r \\ J & j_2 & J_r \end{array}\right\}\left\{\begin{array}{ccc} k & J_s & J^4_r \\ J_r & J & J \end{array}\right\}\left\{\begin{array}{ccc} i & J'_r & J^4_r \\ i' & j_4 & J_s \\ J_i & J^1_r & k \end{array}\right\}$$
$$(1-\delta_{j'3}\delta_{j1}(-1)^{j_1+j_3-J_i}), \tag{E·2}$$

and

$$\mathrm{Coef}_3=\sum_{kJ'_rJ^1_rJ^4_rJ_iJ_rJ_s}\sqrt{[\hat{J}_i\hat{J}'_r\hat{J}_r\hat{J}_s\hat{k}\hat{J}]}(-1)^{i+i'+j_2+J'_r+J'_r}$$
$$\left\{\begin{array}{ccc} j_1 & j_2 & J_1 \\ J & J_2 & J'_r \end{array}\right\}\left\{\begin{array}{ccc} j_3 & j_4 & J_2 \\ J'_r & j_1 & J^1_r \end{array}\right\}\left\{\begin{array}{ccc} i & J^4_r & J'_r \\ J & j_1 & J_r \end{array}\right\}\left\{\begin{array}{ccc} k & J_s & J^4_r \\ J_r & J & J \end{array}\right\}\left\{\begin{array}{ccc} i & J'_r & J^4_r \\ i' & j_4 & J_s \\ J_i & J^1_r & k \end{array}\right\}$$
$$(1-\delta_{j'2}\delta_{j3}(-1)^{j_2+j_3-J_i}). \tag{E·3}$$

By using these normalization coefficients we obtain the CFT for the three partitions by diagonalizing the following matrix:

$$\left(\begin{array}{c|c|c} \mathrm{Coef}_1{*}\mathrm{Coef}_1 & \mathrm{Coef}_1{*}\mathrm{Coef}_2 & \mathrm{Coef}_1{*}\mathrm{Coef}_3 \\ \hline \mathrm{Coef}_2{*}\mathrm{Coef}_1 & \mathrm{Coef}_2{*}\mathrm{Coef}_2 & \mathrm{Coef}_2{*}\mathrm{Coef}_3 \\ \hline \mathrm{Coef}_3{*}\mathrm{Coef}_1 & \mathrm{Coef}_3{*}\mathrm{Coef}_2 & \mathrm{Coef}_3{*}\mathrm{Coef}_3 \end{array}\right)\begin{pmatrix} |([a^\dagger_{j_1}a^\dagger_{j_2}]^{J_r}[a^\dagger_{j_3}a_{j_4}]^{J_s})^J\rangle \\ |([a^\dagger_{j_3}a^\dagger_{j_2}]^{J_r}[a^\dagger_{j_1}a_{j_4}]^{J_s})^J\rangle \\ |([a^\dagger_{j_1}a^\dagger_{j_3}]^{J_r}[a^\dagger_{j_2}a_{j_4}]^{J_s})^J\rangle \end{pmatrix}$$
$$=\begin{pmatrix} {}^5V^{\dagger(3,1)}_J(\alpha_2J_1|\}\lambda_1\epsilon_1J_r\bar{\epsilon_1}J_s)\cdot{}^5V^{(3,1)}_J(\alpha_2J_1|\}\lambda_1\epsilon_1J_r\bar{\epsilon_1}J_s) \\ {}^5V^{\dagger(3,1)}_J(\alpha_2J_1|\}\lambda_2\epsilon_2J_r\bar{\epsilon_2}J_s)\cdot{}^5V^{(3,1)}_J(\alpha_2J_1|\}\lambda_2\epsilon_2J_r\bar{\epsilon_2}J_s) \\ {}^5V^{\dagger(3,1)}_J(\alpha_2J_1|\}\lambda_3\epsilon_3J_r\bar{\epsilon_3}J_s)\cdot{}^5V^{(3,1)}_J(\alpha_2J_1|\}\lambda_3\epsilon_3J_r\bar{\epsilon_3}J_s) \end{pmatrix}\begin{pmatrix} |([a^\dagger_{j_1}a^\dagger_{j_2}]^{J_r}[a^\dagger_{j_3}a_{j_4}]^{J_s})^J\rangle \\ |([a^\dagger_{j_3}a^\dagger_{j_2}]^{J_r}[a^\dagger_{j_1}a_{j_4}]^{J_s})^J\rangle \\ |([a^\dagger_{j_1}a^\dagger_{j_3}]^{J_r}[a^\dagger_{j_2}a_{j_4}]^{J_s})^J\rangle \end{pmatrix}. \tag{E·4}$$

The CFC coefficients associated to the u operators are derived within the same computational method introduced for the π operators; the normalization factors $(c_{\mu_i};\mu_i=4,5,6)$ are given below:

$$\mathrm{Coef}_4=\sum_{kJ'_rJ^1_rJ^2_rJ_iJ_rJ_s}\sqrt{[\hat{J}_1\hat{J}_2\hat{J}^1_r\hat{J}_s\hat{J}_i\hat{k}\hat{J}]}(-1)^{i+j_1+j_3+J^2_r+J_2+J_r+J_s+J+1}$$
$$\left\{\begin{array}{ccc} j_1 & j_2 & J_1 \\ J'_r & j_4 & J^1_r \end{array}\right\}\left\{\begin{array}{ccc} j_3 & j_4 & J_2 \\ J_1 & J & J'_r \end{array}\right\}\left\{\begin{array}{ccc} i & j & J_i \\ k & J^1_r & J^2_r \end{array}\right\}\left\{\begin{array}{ccc} i & J^2_r & J^1_r \\ J'_r & j_2 & J_s \end{array}\right\}\left\{\begin{array}{ccc} J_s & J_r & J \\ J^2_r & j_4 & k \\ J'_r & j_3 & J \end{array}\right\}, \tag{E·5}$$

$$\mathrm{Coef}_5=\mathrm{Coef}_4*(-1)^{j_1+j_2-J_1}\text{ with }(j_1\rightarrow j_2), \tag{E·6}$$

and

$$\text{Coef}_6 = \sum_{kJ'_rJ_r} \sqrt{[\hat{k}\hat{J}]}(-1)^{j_3+j_4+1+k+J_1+J_r} \left\{ \begin{array}{ccc} J_r & k & J_2 \\ J & J_1 & J'_r \end{array} \right\} \delta_{J_sJ_1}. \tag{E·7}$$

By using these normalization coefficients we obtain the CFT for the three partitions by diagonalizing the following matrix:

$$\begin{pmatrix} \text{Coef}_4{*}\text{Coef}_4 & \text{Coef}_4{*}\text{Coef}_5 & \text{Coef}_4{*}\text{Coef}_6 \\ \text{Coef}_5{*}\text{Coef}_4 & \text{Coef}_5{*}\text{Coef}_5 & \text{Coef}_5{*}\text{Coef}_6 \\ \text{Coef}_6{*}\text{Coef}_4 & \text{Coef}_6{*}\text{Coef}_5 & \text{Coef}_6{*}\text{Coef}_6 \end{pmatrix} \begin{pmatrix} |([a^\dagger_{j_1}a_{j_4}]^{J_r}[a^\dagger_{j_2}a^\dagger_{j_3}]^{J_s})^J\rangle \\ |([a^\dagger_{j_2}a_{j_4}]^{J_r}[a^\dagger_{j_1}a^\dagger_{j_3}]^{J_s})^J\rangle \\ |([a^\dagger_{j_3}a_{j_4}]^{J_r}[a^\dagger_{j_1}a^\dagger_{j_2}]^{J_s})^J\rangle \end{pmatrix}$$
$$= \begin{pmatrix} {}^5U^{\dagger(3,1)}_J(\alpha_2J_1|\}\mu_1\eta_1J_r\bar{\eta_1}J_s)\cdot{}^5U^{(3,1)}_J(\alpha_2J_1|\}\mu_1\eta_1J_r\bar{\eta_1}J_s) \\ {}^5U^{\dagger(3,1)}_J(\alpha_2J_1|\}\mu_2\eta_2J_r\bar{\eta_2}J_s)\cdot{}^5U^{(3,1)}_J(\alpha_2J_1|\}\mu_2\eta_2J_r\bar{\eta_2}J_s) \\ {}^5U^{\dagger(3,1)}_J(\alpha_2J_1|\}\mu_3\eta_3J_r\bar{\eta_3}J_s)\cdot{}^5U^{(3,1)}_J(\alpha_2J_1|\}\mu_3\eta_3J_r\bar{\eta_3}J_s) \end{pmatrix} \begin{pmatrix} |([a^\dagger_{j_1}a_{j_4}]^{J_r}[a^\dagger_{j_2}a^\dagger_{j_3}]^{J_s})^J\rangle \\ |([a^\dagger_{j_2}a_{j_4}]^{J_r}[a^\dagger_{j_1}a^\dagger_{j_3}]^{J_s})^J\rangle \\ |([a^\dagger_{j_3}a_{j_4}]^{J_r}[a^\dagger_{j_1}a^\dagger_{j_2}]^{J_s})^J\rangle \end{pmatrix}. \tag{E·8}$$

Appendix F

—— A Numerical Application of the CFT ——

In this appendix we apply the method of the previous appendix to calculate the CFC for a $(1d_{\frac{5}{2}}2s_{\frac{1}{2}})^2(d_{\frac{3}{2}}p^{-1}_{\frac{3}{2}})^1$-(3p1h) CMWFs formed by coupling two particles assumed to be in the $1d_{\frac{5}{2}}$ and $2s_{\frac{1}{2}}$ single-particle shell model states to the $d_{\frac{3}{2}}p^{-1}_{\frac{3}{2}}$ p-h pair. By using Eq. (E·1) we write for Coef_1:

$$\text{Coef}_1 = -\sum_{J_r} 3. \left\{ \begin{array}{ccc} J_r & 1 & 2 \\ 1 & 1 & 1 \end{array} \right\} \tag{F·1}$$

which by restricting the quantum numbers to $k = 1$ for $(J_1 = 2, J_2 = J_s = 1, J = 1, J_r = 2)$ give the cases of Table III. The Coef_2 given in Eq. (E·2) assumes for $k = 1$ the form

$$\text{Coef}_2 = \sum_{J'_rJ^1_rJ^4_rJ_rJ_s} (\hat{J}'_r\hat{J}^4_r)[5\cdot 3\cdot 9\hat{J}_i\hat{J}^1_r\hat{J}_s]^{\frac{1}{2}}(-1)^{\frac{3}{2}+J'_r+J^1_r+J_r}$$
$$\left\{ \begin{array}{ccc} \frac{5}{2} & \frac{1}{2} & 2 \\ 1 & 1 & J'_r \end{array} \right\} \left\{ \begin{array}{ccc} \frac{3}{2} & \frac{3}{2} & 1 \\ J'_r & \frac{5}{2} & J^1_r \end{array} \right\} \left\{ \begin{array}{ccc} \frac{1}{2} & J^4_r & J'_r \\ 1 & \frac{1}{2} & J_r \end{array} \right\} \left\{ \begin{array}{ccc} 1 & J_s & J^4_r \\ J_r & 1 & 1 \end{array} \right\} \left\{ \begin{array}{ccc} \frac{1}{2} & J'_r & J^4_r \\ \frac{5}{2} & \frac{3}{2} & J_s \\ J_i & J^1_r & 1 \end{array} \right\}. \tag{F·2}$$

In Eq. (F·2) the range of the indices in the sum is running over the following possibilities:

$J'_r = 3/2$	$J'_r = 5/2$	$J'_r = 7/2$
$J^1_r = 0, 1, 2, 3$	$J^1_r = 1, 2, 3, 4$	$J^1_r = 2, 3, 4, 5$
$J_s = 0, 1, 2, 3$	$J_s = 0, 1, 2, 3$	$J_s = 0, 1, 2, 3$
$J^4_r = 1, 2, 3, 4$	$J^4_r = 0, 1, 2, 3, 4, 5$	$J^4_r = 2, 3, 4, 5$
$J_r = 0, 1, 2, 3, 4, 5$	$J_r = 0, 1, 2, 3, 4, 5$	$J_r = 0, 1, 2, 3, 4, 5$
$J_i = 1, 2, 3, 4$	$J_i = 1, 2, 3, 4$	$J_i = 1, 2, 3, 4$

(F·3)

By summing over all the possible cases we obtain for this special case the Coef_2 given in Table IV. The Coef_3 coefficients are given in Eq. (E·3) and for $k = 1$ we

obtain

$$\begin{aligned}&\mathrm{Coef}_3\\&=\sum_{J_r' J_r^1 J_r^4 J_r J_s}[\hat{J}_i\hat{J}_r'\hat{J}_r\hat{J}_s 3.3]^{\frac{1}{2}}(-1)^{\frac{1}{2}+J_r'+J_r^1}\\&\left\{\begin{array}{ccc}\frac{5}{2}&\frac{1}{2}&2\\1&1&J_r'\end{array}\right\}\left\{\begin{array}{ccc}\frac{3}{2}&\frac{3}{2}&1\\J_r'&\frac{5}{2}&J_r^1\end{array}\right\}\left\{\begin{array}{ccc}\frac{1}{2}&J_r^4&J_r'\\J&\frac{5}{2}&J_r\end{array}\right\}\left\{\begin{array}{ccc}1&J_r^3&J_r^4\\J_r&1&1\end{array}\right\}\left\{\begin{array}{ccc}\frac{1}{2}&J_r'&J_r^4\\\frac{3}{2}&\frac{3}{2}&J_s\\J_i&J_r^1&1\end{array}\right\}.\end{aligned}\tag{F·4}$$

For this special example the calculated Coef_3 are given in Table III. We see that the matrix we have to diagonalize in order to get the cluster coefficients is of the order of eight. By introducing the coefficient of Tables III and IV in Eq. (E·4) and by diagonalizing the derived matrix we get the V-CFC given in Table V. Analogous calculations can be performed for the u operators. The Coef_4 given in Eq. (E·5) assumes for $k=1$ the form

$$\begin{aligned}\mathrm{Coef}_4=&\sum_{k J_r' J_r^1 J_r^2 J_i J_r J_s}[\hat{J}_1\hat{J}_2\hat{J}_r^1\hat{J}_s\hat{J}_i\hat{k}\hat{J}]^{\frac{1}{2}}(-1)^{i+j_1+j_3+J_r^2+J_2+J_r+J_s+J+1}\\&\left\{\begin{array}{ccc}\frac{5}{2}&\frac{1}{2}&2\\J_r'&\frac{3}{2}&J_r^1\end{array}\right\}\left\{\begin{array}{ccc}\frac{3}{2}&\frac{3}{2}&1\\2&1&J_r'\end{array}\right\}\left\{\begin{array}{ccc}\frac{3}{2}&\frac{1}{2}&J_i\\1&J_r^1&J_r^2\end{array}\right\}\left\{\begin{array}{ccc}\frac{3}{2}&J_r^2&J_r^1\\J_r'&\frac{1}{2}&J_s\end{array}\right\}\left\{\begin{array}{ccc}J_s&cJ_s&1\\J_r^2&\frac{3}{2}&1\\J_r'&\frac{3}{2}&1\end{array}\right\}.\end{aligned}\tag{F·5}$$

By summing over all possible partitions we obtain the Coef_4 coefficients which are given in Table VI. For the Coef_5 we use the previous formula by replacing $j_1\rightarrow j_2$, and we calculated coefficients given in Table VI. The Coef_6 are calculated from Eq. (E·7) which in this special example takes the form

$$\mathrm{Coef}_6=\sum_{J_r}3.*(-1)^{1+2+J_r}\left\{\begin{array}{ccc}J_r&1&1\\1&2&1\end{array}\right\}.\tag{F·6}$$

Now since $J_r=1,2$ we have for Coef_6 the coefficients given in Table VII. By using the coefficients $\mathrm{Coef}_i, i=4,5,6$ we derive the CFC for the U operators given in Table VIII. By recalling that the pair coupled to J_r is active we write for the matrix elements calculated in the $((d_{\frac{5}{2}}s_{\frac{1}{2}})^2(d_{\frac{3}{2}}p_{\frac{3}{2}}^{-1})^1)^1$ CMWF the following value:

$$\begin{aligned}&\langle d_{\frac{5}{2}}s_{\frac{1}{2}}d_{\frac{3}{2}}p_{\frac{3}{2}}^{-1}|v(r)|d_{\frac{5}{2}}s_{\frac{1}{2}}d_{\frac{3}{2}}p_{\frac{3}{2}}^{-1}\rangle_a^1\\&=(0.0617)^2\langle d_{\frac{5}{2}}s_{\frac{1}{2}}|v_{pp}(r)|d_{\frac{5}{2}}s_{\frac{1}{2}}\rangle_a^2+(0.0589)^2\langle d_{\frac{3}{2}}s_{\frac{1}{2}}|v_{pp}(r)|d_{\frac{3}{2}}s_{\frac{1}{2}}\rangle_a^2\\&+(-0.2088)^2\langle d_{\frac{3}{2}}s_{\frac{1}{2}}|v_{pp}(r)|d_{\frac{3}{2}}s_{\frac{1}{2}}\rangle_a^2+(0.2352)^2\langle d_{\frac{3}{2}}s_{\frac{1}{2}}|v_{pp}(r)|d_{\frac{3}{2}}s_{\frac{1}{2}}\rangle_a^2\\&+(0.6029)^2\langle d_{\frac{5}{2}}d_{\frac{3}{2}}|v_{pp}(r)|d_{\frac{5}{2}}d_{\frac{3}{2}}\rangle_a^2+(-0.3346)^2\langle d_{\frac{5}{2}}d_{\frac{3}{2}}|v_{pp}(r)|d_{\frac{5}{2}}d_{\frac{3}{2}}\rangle_a^2\\&+(0.6466)^2\langle d_{\frac{5}{2}}d_{\frac{3}{2}}|v_{pp}(r)|d_{\frac{5}{2}}d_{\frac{3}{2}}\rangle_a^3+(0.0908)^2\langle s_{\frac{1}{2}}p_{\frac{3}{2}}|v_{ph}(r)|s_{\frac{1}{2}}p_{\frac{3}{2}}\rangle_a^2\\&+(-0.1504)^2\langle s_{\frac{1}{2}}p_{\frac{3}{2}}|v_{ph}(r)|s_{\frac{1}{2}}p_{\frac{3}{2}}\rangle_a^2+(0.4022)^2\langle d_{\frac{3}{2}}p_{\frac{3}{2}}|v_{ph}(r)|d_{\frac{3}{2}}p_{\frac{3}{2}}\rangle_a^1\\&+(-0.3278)^2\langle d_{\frac{3}{2}}p_{\frac{3}{2}}|v_{ph}(r)|d_{\frac{3}{2}}p_{\frac{3}{2}}\rangle_a^2+(0.7873)^2\langle d_{\frac{3}{2}}p_{\frac{3}{2}}|v_{ph}(r)|d_{\frac{3}{2}}p_{\frac{3}{2}}\rangle_a^2\\&+(0.2094)^2\langle d_{\frac{5}{2}}p_{\frac{3}{2}}|v_{ph}(r)|d_{\frac{5}{2}}p_{\frac{3}{2}}\rangle_a^1+(0.1883)^2\langle d_{\frac{5}{2}}p_{\frac{3}{2}}|v_{ph}(r)|d_{\frac{5}{2}}p_{\frac{3}{2}}\rangle_a^2.\end{aligned}\tag{F·7}$$

One has to note that in the ladder approximations only the first seven terms of Eq. (F·7) contribute to the matrix elements.

Table III. Coef_1 as functions of J_r and J_s.

J_r	J_s	Coef_1
2	1	0.0671

Table IV. Coef_2 and Coef_3 as functions of J_r and J_s.

J_r	J_s	Coef_2	Coef_3
2	1	-0.5909001110^{-01}	-0.1050328410^{-02}
2	2	-0.3650307710^{-02}	0.1547969910^{-02}
2	3	-0.2182041110^{-01}	-
3	2	-	-0.1612873310^{-02}

Table V. Cluster factorization coefficients $V_1^{3,1}([d_{\frac{5}{2}}s_{\frac{1}{2}}J_1 = 2][d_{\frac{3}{2}}p_{\frac{3}{2}}^{-1}J_2 = 1]\}[j_ij_jJ_r][j_lj_m^{-1}J_s])$ calculated for the seven allowed partitions and related CMWFs.

λ_i	J_r	J_s	CFC	wave function
1	2	1	0.0617	$\vert((d_{\frac{5}{2}}s_{\frac{1}{2}})^{J_r=2}(d_{\frac{3}{2}}p_{\frac{3}{2}}^{-1})^{J_s=1})^1\rangle$
2	2	1	0.0589	$\vert((d_{\frac{3}{2}}s_{\frac{1}{2}})^{J_r=2}(d_{\frac{5}{2}}p_{\frac{3}{2}}^{-1})^{J_s=1})^1\rangle$
3	2	2	-0.2088	$\vert((d_{\frac{3}{2}}s_{\frac{1}{2}})^{J_r=2}(d_{\frac{5}{2}}p_{\frac{3}{2}}^{-1})^{J_s=2})^1\rangle$
4	2	3	0.2352	$\vert((d_{\frac{3}{2}}s_{\frac{1}{2}})^{J_r=2}(d_{\frac{5}{2}}p_{\frac{3}{2}}^{-1})^{J_s=3})^1\rangle$
5	2	1	0.6029	$\vert((d_{\frac{5}{2}}d_{\frac{3}{2}})^{J_r=2}(s_{\frac{1}{2}}p_{\frac{3}{2}}^{-1})^{J_s=1})^1\rangle$
6	2	2	-0.3346	$\vert((d_{\frac{5}{2}}d_{\frac{3}{2}})^{J_r=2}(s_{\frac{1}{2}}p_{\frac{3}{2}}^{-1})^{J_s=2})^1\rangle$
7	3	2	0.6466	$\vert((d_{\frac{5}{2}}d_{\frac{3}{2}})^{J_r=3}(s_{\frac{1}{2}}p_{\frac{3}{2}}^{-1})^{J_s=2})^1\rangle$

Table VI. Coef_4 and Coef_5 as functions of J_r and J_s.

J_r	J_s	Coef_4	Coef_5
2	1	0.3199068110^{-01}	0.11957474
2	2	0.5368016710^{-01}	0.3506421710^{-01}
2	3	-	-0.10351003

Table VII. Coef_6 as functions of J_r and J_i.

J_r	J_s	Coef_6
1	2	0.5000
2	2	0.0671

Table VIII. Cluster factorization coefficients $U_1^{3,1}([d_{\frac{5}{2}}s_{\frac{1}{2}}J_1 = 2][d_{\frac{3}{2}}p_{\frac{3}{2}}^{-1}J_2 = 1]\}[j_ij_j^{-1}J_r][j_lj_mJ_s])$ calculated for the seven allowed partitions and related CMWFs.

μ_i	J_r	J_s	CFC	wave function
1	1	2	0.0908	$\vert((s_{\frac{1}{2}}p_{\frac{3}{2}}^{-1})^{J_r=2}(d_{\frac{5}{2}}d_{\frac{3}{2}})^{J_s=1})^1\rangle$
2	2	2	-0.1574	$\vert((s_{\frac{1}{2}}p_{\frac{3}{2}}^{-1})^{J_r=2}(d_{\frac{5}{2}}d_{\frac{3}{2}})^{J_s=2})^1\rangle$
3	1	2	0.4022	$\vert((d_{\frac{3}{2}}p_{\frac{3}{2}}^{-1})^{J_r=1}(d_{\frac{5}{2}}s_{\frac{1}{2}})^{J_s=2})^1\rangle$
4	2	2	-0.3278	$\vert((d_{\frac{3}{2}}p_{\frac{3}{2}}^{-1})^{J_r=2}(d_{\frac{5}{2}}s_{\frac{1}{2}})^{J_s=2})^1\rangle$
5	2	3	0,7873	$\vert((d_{\frac{3}{2}}p_{\frac{3}{2}}^{-1})^{J_r=2}(d_{\frac{5}{2}}s_{\frac{1}{2}})^{J_s=3})^1\rangle$
6	1	2	0.2094	$\vert((d_{\frac{5}{2}}p_{\frac{3}{2}}^{-1})^{J_r=1}(d_{\frac{3}{2}}s_{\frac{1}{2}})^{J_s=2})^1\rangle$
7	2	2	0.1883	$\vert((d_{\frac{5}{2}}p_{\frac{3}{2}}^{-1})^{J_r=2}(d_{\frac{3}{2}}s_{\frac{1}{2}})^{J_s=2})^1\rangle$

Table IX. List of the most significant components of the ground state 0^+, $T = 1$ wave function of ^{6}He with $E = -24.97$ MeV.

Spect. fact.	$1p_{\frac{3}{2}}1p_{\frac{3}{2}}$	$1p_{\frac{1}{2}}1p_{\frac{1}{2}}$	$(1p_{\frac{3}{2}}1d_{\frac{5}{2}})^{2,1}(1p_{\frac{3}{2}}1s_{\frac{1}{2}}^{-1})^{2,0}$	$(1p_{\frac{3}{2}}1d_{\frac{5}{2}})^{2,1}(1p_{\frac{3}{2}}1s_{\frac{1}{2}}^{-1})^{2,1}$
0.9370	0.9680	0.1816	−0.1145	0.0628

Table X. List of the most significant components of the ground state 1^+, $T = 0$ wave function of ^{6}Li calculated within the small base with $E = -19.30$ MeV.

Spect. fact.	$1p_{\frac{3}{2}}1p_{\frac{3}{2}}$	$1p_{\frac{3}{2}}1p_{\frac{1}{2}}$	$1p_{\frac{1}{2}}1p_{\frac{1}{2}}$	$1d_{\frac{5}{2}}1d_{\frac{3}{2}}$	$(1p_{\frac{3}{2}}1d_{\frac{5}{2}})^{2,0}(1p_{\frac{3}{2}}1s_{\frac{1}{2}}^{-1})^{1,0}$
0.7649	0.8746	0.4559	−.1009	0.0385	0.0261

Spect. fact.	$(1p_{\frac{1}{2}}2s_{\frac{1}{2}})^{0,0}(1p_{\frac{3}{2}}1s_{\frac{1}{2}}^{-1})^{1,0}$
0.7649	−0.0111

Table XI. List of the most significant components of the ground state 1^+, $T = 0$ wave function of ^{6}Li calculated within the large base with $E = -21.2$ MeV.

Spect. fact.	$1p_{\frac{3}{2}}1p_{\frac{3}{2}}$	$1p_{\frac{3}{2}}1p_{\frac{1}{2}}$	$1d_{\frac{5}{2}}1d_{\frac{5}{2}}$	$1d_{\frac{5}{2}}1d_{\frac{3}{2}}$	$(1p_{\frac{3}{2}}1d_{\frac{5}{2}})^{2,0}(1p_{\frac{3}{2}}1s_{\frac{1}{2}}^{-1})^{1,0}$
0.6427	0.8017	0.4906	−0.0636	−0.1155	0.0653

Spect. fact.	$(1p_{\frac{1}{2}}2s_{\frac{1}{2}})^{0,0}(1p_{\frac{3}{2}}1s_{\frac{1}{2}}^{-1})^{1,0}$
0.6427	0.03725

Appendix G

—— Spectroscopic Factors of the Dressed Wave Functions ——

The spectroscopic factor of the ground states of mass $A = 6$ isotopes is defined by

$$S_{p_{\frac{3}{2}}p_{\frac{3}{2}}} = \langle \Phi_{2p} | a^\dagger_{p_{\frac{3}{2}}} a^\dagger_{p_{\frac{3}{2}}} | 0 \rangle. \tag{G·1}$$

The spectroscopic factor for the two neutrons in the ^{6}He together with the more significant components of the dressed $J = 0^+$, $T = 1$ wave function of the ground state are given in Table IX. For ^{6}Li the spectroscopic factor and the more significant components of the $J = 1^+$, $T = 0$ ground state wave function are given in Table X for the small configuration space. Corresponding values calculated with the large configuration space are given in Table XI.

Appendix H

—— Charge Distribution for Two Correlated Particles ——

In this appendix we give the difference between the distribution calculated for two non-correlated particles in shell model states and that calculated for two dressed (correlated) particles. In the shell model the distributions are evaluated by using the expectation values of the operators:

$$\rho(r) = \sum_\alpha \langle \alpha | \delta(r - r_\alpha) | \alpha \rangle a^\dagger_\alpha a_\alpha \tag{H·1}$$

between the two particle shell model states:

$$[(j_1 j_2)^J] = a^\dagger_{j_1} a^\dagger_{j_2} |0\rangle. \tag{H·2}$$

By performing small algebra we obtain

$$\rho(r) = \rho_{j_1}(r) + \rho_{j_2}(r), \tag{H·3}$$

where ρ_{j_i} is the single-particle distribution. This distribution is valid only in an extreme single-particle model, i.e., Shell Model, Hartree-Fock and mean field theories. In the BDCM the effect of the long-range correlation must be included consistently in the calculation of the densities. We need therefore to calculate the distribution starting from the correlated particle pair given below:

$$\tilde{\Psi}_{12} \equiv e^S \Psi_{12} = (1 + S_1 + S_2 + S_3 + \cdots)\Psi_{12}, \tag{H·4}$$

where the $S_i, i = 1, 2 \cdots$ are the correlation operators of the i-th order. Within our approximation the density should therefore be calculated from the model CMWFs:

$$\tilde{\Psi}_{12} = \sum_{ij} \chi_{ij} \Psi_{ij} + \sum_{ijkl} \chi_{ijkl} \Psi_{ij} \Psi_{kl}. \tag{H·5}$$

By using the amplitudes of Eq. (2·21) and the CFC of Eq. (2·22) we derive, discarding the isospin quantum numbers, the following equation:

$$\begin{aligned}
\rho^J(R) = \Bigg(& \sum_{\alpha_1} \chi^2_{\alpha_1} \sum_{nlNL\lambda} \langle n_1 l_1 n_2 l_2 \lambda | \} nlNL\lambda \rangle^2 \text{angcoef}(\alpha_1 \alpha_1 \lambda\lambda J) \Phi^2_{NL}(R) \\
& + 2 \sum_{\alpha_1 \alpha_2} \chi_{\alpha_1} \chi_{\alpha_2} \Bigg(\sum_{J_r \epsilon_i} {}^5V^{(3,1)}_J (\alpha_2 J_1 J_2 | \} \epsilon_i J_r \bar{\epsilon}_i J_s) \\
& \cdot \sum_{nlNL\lambda\lambda'} \langle n_1 l_1 n_2 l_2 \lambda | \} nlNL\lambda \rangle \langle n_i l_i n'_i l'_i \lambda' | \} nlNL\lambda' \rangle \text{angcoef}(\alpha_1 \epsilon_i \lambda\lambda' J_r) \Phi^2_{NL}(R) \\
& + \sum_{J_r \alpha_i} {}^5U^{(3,1)}_J (\alpha_2 J_1 J_2 | \} \alpha_i J_r \bar{\alpha}_i J_s) \\
& \cdot \sum_{nlNL\lambda\lambda'} \langle n_1 l_1 n_2 l_2 \lambda | \} nlNL\lambda \rangle \langle n_i l_i n'_i l'_i \lambda' | \} nlNL\lambda' \rangle \text{angcoef}(\alpha_1 \alpha_i \lambda\lambda' J_r) \Phi^2_{NL}(R) \Bigg) \\
& + \sum_{\alpha_2 \beta_2} \chi_{\alpha_2} \chi_{\beta_2} \Bigg(\sum_{J_r J_{r'} \epsilon_i \epsilon_j} {}^5V^{\dagger(3,1)}_J (\alpha_2 J_1 J_2 | \} \epsilon_i J_r \bar{\epsilon}_i J_s) {}^5V^{(3,1)}_J (\beta_2 J_1 J_2 | \} \epsilon_j J'_r \bar{\epsilon}_j J_s) \\
& \cdot \sum_{nlNL\lambda\lambda'} \langle n_i l_i n'_i l'_i \lambda | \} nlNL\lambda \rangle \langle n_j l_j n'_j l'_j \lambda' | \} nlNL\lambda' \rangle \text{angcoef}(\epsilon_i \epsilon_j \lambda\lambda' J) \Phi^2_{NL}(R) \\
& + \sum_{J_r J_{r'} \beta_i \beta_j} {}^5U^{\dagger(3,1)}_J (\alpha_2 J_1 J_2 | \} \beta_i J_r \bar{\beta}_i J_s) {}^5U^{(3,1)}_J (\beta_2 J_1 J_2 | \} \beta_j J'_r \bar{\beta}_j J_s) \\
& \cdot \sum_{nlNL\lambda\lambda'} \langle n_i l_i n'_i l'_i \lambda | \} nlNL\lambda \rangle \langle n_j l_j n'_j l'_j \lambda' | \} nlNL\lambda' \rangle \text{angcoef}(\beta_i \beta_j \lambda\lambda' J) \Phi^2_{NL}(R) \Bigg) \Bigg),
\end{aligned} \tag{H·6}$$

where R is the center of mass of the dressed particles, $(nlNL)$ the relative and center of mass angular momenta of the $(\alpha_i, \beta_i, \epsilon_i)$ pairs, and the brackets are the Moshinski

brackets.[38),39)] The χ_{α_1} are the shell model amplitudes and the χ_{α_2} the (3p1h) amplitudes. The angcoef's of Eq. (2·37) are angular momentum transformation coefficients between the (jj) and the (ls) coupling given below:

$$\begin{aligned}
&\text{angcoef}(\alpha_1\alpha_1'\lambda\lambda' J)\\
&= (\tfrac{1}{2}\tfrac{1}{2}s, l_1 l_2\lambda|\}(\tfrac{1}{2}l_1)j_1, (\tfrac{1}{2}l_2)j_2, \lambda)(\tfrac{1}{2}\tfrac{1}{2}s', l_1' l_2'\lambda'|\}(\tfrac{1}{2}l_1')j_1', (\tfrac{1}{2}l_2')j_2', \lambda')\\
&= \sqrt{[\hat{j_1}\hat{j_2}]}\hat{\lambda}(-1)^{\lambda}
\left\{ \begin{array}{ccc} \frac{1}{2} & \frac{1}{2} & s \\ l_1 & l_2 & \lambda \\ j_1 & j_2 & J_{12} \end{array} \right\}
\left\{ \begin{array}{ccc} L & l & \lambda \\ s & J_{12} & J \end{array} \right\}\\
&\sqrt{[\hat{j_1'}\hat{j_2'}]}\hat{\lambda'}(-1)^{\lambda'}
\left\{ \begin{array}{ccc} \frac{1}{2} & \frac{1}{2} & s' \\ l_1' & l_2' & \lambda' \\ j_1' & j_2' & J_{1'2'} \end{array} \right\}
\left\{ \begin{array}{ccc} L' & l' & \lambda' \\ s' & J_{1'2'} & J \end{array} \right\}. \qquad \text{(H·7)}
\end{aligned}$$

The angcoef$(\alpha_1\epsilon_1\lambda\lambda' J)$, angcoef$(\epsilon_1\epsilon_1'\lambda\lambda' J)$, and angcoef$(\beta_1\beta_1'\lambda\lambda' J)$ coefficients have a form analogous to that of Eq. (H·7). The symbols α_1, α_1', β_1, β_1', and ϵ_1, ϵ_1' are given below:

$$\begin{array}{lcl}
\alpha_1 & \longrightarrow & \text{two valence particles,}\\
\alpha_1', \beta_1, \text{ and } \beta_1' & \longrightarrow & \text{two particles from the (3p1h) CMWFs,}\\
\epsilon_1 \text{ and } \epsilon_1' & \longrightarrow & \text{particle-hole form the (3p1h) CMWFs.}
\end{array} \qquad \text{(H·8)}$$

The effect of the folded diagrams on the calculated distributions is given in Fig. 1 where we compare the correlated distribution of ^{6}He calculated with Eq. (H·4) by neglecting the particle-hole diagrams with that calculated by including also these diagrams. Analogous calculations will be performed for any operators. Until now this effect has not been considered by the other theoretical models. The translational invariant density of Ref. 40) is derived by assuming that the wave functions of the nuclei are given in the terms of non-correlated Slater determinants.

References

1) F. Villars, *Proc. Enrico Fermi Int. School of Physics XXII* (Academic Press, N.Y., 1961).
2) C. M. Shakin and Y. R. Waghmare, Phys. Rev. Lett. **16** (1966), 403.
   C. M. Shakin, Y. R. Waghmare and M. H. Hull, Phys. Rev. **161** (1967), 1006.
3) M. Tomaselli, L. C. Liu, S. Fritzsche, T. Kühl and D. Ursescu, Nucl. Phys. A **738** (2004), 216.
   M. Tomaselli, L.C. Liu, S. Fritzsche and T. Kühl, J. of Phys. G **30** (2004), 999.
4) K. A. Brückner, *The Many Body Problem* (John Wiley and Sons, New York, 1959).
5) T. T. S. Kuo and E. Osnes, "Folded-Diagrams Theory of the Effective Interaction in Atomic Nuclei", *Lecture Notes in Phys.* **366** (Springer, Berlin, 1991).
6) P. Navrátil and B. R. Barrett, Phys. Rev. C **57** (1998), 3119.
   P. Navrátil and E. Caurier, Phys. Rev. C **69** (2004), 014311.
7) I. Stancu, B. R. Barrett, P. Navrátil and J. P. Vary, Phys. Rev. C **71** (2005), 044325.
8) Y. KanadaEn'yo and H. Horiuchi, Phys. Rev. C **55** (1997), 2860.
9) S. C. Pieper and R. B. Wiringa, Annu. Rev. Part. Sci. **51** (2001), 53.
10) L.-B. Wang, P. Müller, V. Bailey et al., Phys. Rev. Lett. **93** (2004), 142501.
11) J. Würzer and H. M. Hofmann, Phys. Rev. C **55** (1997), 688.
12) S. Funada, H. Kaneyama and Y. Sakuragi, Nucl. Phys. A **575** (1994), 93.
13) K. Varga, Y. Suzuki and Y. Ohbayasi, Phys. Rev. C **50** (1994), 189.
14) M. Tomaselli, T. Kühl, W. Nörtershäuser, G. Ewald, R. Sanchez, S. Fritzsche and G. S. Karshenboim, Can. J. Phys. **80** (2002), 1347.
15) G. Ewald, W. Nörtershäuser, A. Dax et al., Phys. Rev. Lett. **93** (2004), 113002.
   B. A. Bushaw, W. Nörtershäuser, G. Ewald et al., Phys. Rev. Lett. **91** (2003), 043004.

R. Sánchez, W. Nörtershäuser, G. Ewald, D. Albers, J. Behr, P. Bricault, B. A. Bushaw, A. Dax, J. Dilling, M. Dombsky, G. W. F. Drake, S. Götte, R. Kirchner, H.-J. Kluge, T. Kühl, J. Lassen, C. D. P. Levy, M. R. Pearson, E. J. Prime, V. Ryjkov, A. Wojtaszek, Z.-C. Yan and C. Zimmerman, Phys. Rev. Lett. **96** (2005), 033002.
16) Z.-C. Yan and G. W. F. Drake, Phys. Rev. A **66** (2002), 042504.
17) G. C. Li, I. Sick, R. R. Whitney and M. R. Yearian, Nucl. Phys. A **162** (1971), 583.
18) P. Aufmuth, J. of Phys. B **15** (1982), 3127.
19) M. Tomaselli, Can. J. Phys. **83** (2005), 467.
20) M. Anguiano and G. Co, J. of Phys. G **27** (2001), 2109.
21) G. A. Lalazissis and S. E. Massen, nucl-th/9601014.
22) O. Bohigas and S. Stringari, Phys. Lett. B **95** (1980), 9.
23) H. Noya, A. Arima and H. Horie, Prog. Part. Nucl. Phys. **1** (1958), 41.
24) D. J. Millener and D. Kurath, Nucl. Phys. A **255** (1975), 315.
25) G. E. Brown, *Unified Theory of Nuclear Models* (Amsterdam, North-Holland, 1964).
26) U. Fano and G. Racah, *Irreducible Tensorial Sets* (Academic Press, New York, 1959).
G. Racah, "Group theory and spectroscopy", CERN Report 61-8, Geneve, Schwitzerland (1961).
27) D. R. Tilley, C. M. Cheves, J. L. Gowdin, G. M. Hale et al., Nucl. Phys. A **708** (2002), 3.
D. R. Tilley, J. H. Kelley, J. L. Godwin, D. J. Millener, J. E. Purcell et al., Nucl. Phys. A **745** (2004), 155.
H. Koure and M. Yamada, Nucl. Phys. A **671** (2000), 96.
N. Walet, "Nuclear and Particle Physics", `http://walet.Phy.umist.ac.uk/P615/Notes.pdf` (2003), p. 38.
28) D. C. Zheng, J. P. Vary and B. R. Barrett, Phys. Rev. C **50** (1994), 2841.
29) C. M. Shakin, Y. R. Waghmare, M. Tomaselli and M. H. Hull, Phys. Rev. **161** (1967), 1015.
30) T. T. S. Kuo, H. Müther and K. Amir Azimi-Nili, Nucl. Phys. A **606** (1996), 15.
31) M. F. Jiang, R. Machleidt, D. B. Stout and T. T. S. Kuo, Phys. Rev. C **46** (1992), 910.
M. Lacombe, B. Loiseau J. M. Richard, R. Vinh Mau, J. Côté, P. Pirés and R. de Tourreil, Phys. Rev. C **21** (1980), 861.
R. Machleidt, Adv. Nucl. Phys. **19** (1989), 189.
S. Bogner, T. T. S. Kuo, L. Coraggio, A. Covello and N. Itaco, Phys. Rev. C **65** (2002), 051301(R).
32) E. Baranger and C. W. Lee, Nucl. Phys. **22** (1961), 157.
33) I. Unna and I. Talmi, Phys. Rev. **112** (1958), 452.
34) P. Navrátil and E. W. Ormand, Phys. Rev. C **68** (2003), 034305.
35) F. Aksouh, PHD-Thesys, IPNO-T-03-02, Paris-sud University, Orsay (2002).
36) F. Ajzenberg-Selove, Nucl. Phys. A **490** (1988), 1.
37) B. A. Brown, Prog. Part. Nucl. Phys. **47** (2001), 524.
38) T. A. Brody and M. Moshinski, "Table of Transformation Brackets", Monografias del Instituto de Fisica, Universidad Nacional Autonoma de Mexico (1960).
39) D. Ursescu, M. Tomaselli, T. Kühl and S. Fritzsche, Comput. Phys. Commun. **173** (2005), 140.
40) P. Navrátil, Phys. Rev. C **70** (2004), 014317.